Title: Testing the function of widespread transcription of the testis

Authors

Tomohiro Kumon[1,2], Amelie A Raz[1], Jaclyn M Fingerhut[1,2], Yukiko M Yamashita[1,2,3,4,*]

[1]Whitehead Institute for Biomedical Research

[2]Howard Hughes Medical Institute

[3]Massachusetts Institute of Technology, Cambridge, MA 02142, USA

[4]Lead contact

*Correspondence: yukikomy@wi.mit.edu

SUMMARY

In many organisms including *Drosophila* and mammals, male germ cells, particularly spermatocytes, have one of the most complex transcriptomes, where a large fraction of the genome including noncoding DNA are transcribed. However, significance of this widespread transcription remains enigmatic. Through the study of satellite DNA transcription in *Drosophila* spermatocytes as a representational model for widespread transcription, we propose that transcription is required to remodel chromatin in preparation for sperm DNA packaging. We identified HP2, a known heterochromatin protein, as being required for transcription of AAGAG satellite DNA. HP2 depletion led to retention of heterochromatin marks in post-meiotic spermatids and subsequent failure in histone-to-protamine transition. Strikingly, spermatids with less AAGAG satellite DNA can develop normally even when AAGAG transcription is perturbed by HP2 depletion. Together, we propose that spermatocytes' widespread transcription serves as a mechanism to facilitate remodeling of chromatin to prepare for sperm DNA packaging.

INTRODUCTION

In a broad range of organisms from *Drosophila melanogaster* to *Homo sapiens*, testis is known to have a high-complexity transcriptome, where a large fraction of the genome is transcribed (hereafter 'widespread transcription'), including many protein coding genes and long noncoding RNAs (lncRNAs) as well as repetitive sequences such as transposons and satellite DNA[1-7]. Curiously, a large fraction of protein coding genes expressed in the testis are not translated after being transcribed[8], adding a puzzle to widespread transcription in the testis. Since the initial discovery of untranslated transcripts in testis[9], the functional significance of the widespread transcription in the testis has remained enigmatic. A few models have been proposed to explain such widespread transcription. For example, one model proposed that transcription-coupled DNA repair in male germ cells serves to lower mutation rates of protein coding genes[10 but 11], but it does not explain the significance of transcription of noncoding and repetitive sequences. Others proposed that noncoding transcripts function as lncRNA of yet unknown function during spermatogenesis[2,3], but many of them showed no phenotype upon deletion[2]. Yet another model proposed that transcription is a by-product of generally open chromatin in testis[5]. Hence, there is no consensus model that explains widespread transcription of the testis to date.

Here using transcription of satellite DNA during *Drosophila* spermatogenesis as a model (Figure 1A), we investigated the significance of widespread transcription in the testis. Satellite DNA is noncoding tandem repetitive DNA, and constitutes approximately 30% of the *Drosophila* genome (Figure 1B)[12-14]. We show that satellite DNA is highly transcribed in spermatocytes along with other transcripts, contributing to the widespread transcription[1-4]. We found that a heterochromatin binding protein, HP2, which preferentially binds to AAGAG satellite DNA, is required for its transcription in spermatocytes. HP2 depletion led to subfertility due to defective sperm DNA compaction, associated with aberrant retention of heterochromatin histone mark H3K9me3 and defective incorporation of protamine, the sperm-specific DNA packaging protein[15,16]. Strikingly, we found that defects in sperm DNA compaction upon HP2 depletion correlates with the abundance of AAGAG satellite DNA contained in the haploid spermatid: spermatids with the Y chromosome, which contains much more AAGAG satellite DNA than the X chromosome, were particularly sensitive to HP2 depletion, leading to skewed sex ratio in progeny. Moreover, spermatids containing a chromosome II variant with a minimal amount of AAGAG satellite DNA were more resistant to HP2 depletion, leading to a partial rescue of HP2 depletion phenotype. Taken together, we propose that satellite DNA transcription facilitates opening of heterochromatin, and promotes histone-to-protamine transition. We further propose

that the widespread transcription observed in spermatocytes from broad range of organisms may serve a critical role in chromatin remodeling in preparation of sperm DNA packaging.

RESULTS

Drosophila spermatocytes exhibit widespread transcription

To understand the nature of widespread transcription in *Drosophila* testis, we combined the RNA sequencing and cytological analyses. Previous single-nucleus and single-cell RNA-seq data from *Drosophila* testis revealed the widespread transcription of spermatocytes[1], similar to what has been observed in a broad range of organisms[5-7]. Reanalysis of these RNA sequencing data from the *Drosophila* testis[1] showed that 69% of protein coding genes are expressed in the testis (Figure 1C), which is much higher than somatic tissues[17]. Comparison of transcriptome[1] and proteome[18] further revealed that more than half of transcribed protein-coding genes (i.e., 42.1% of total protein coding genes) are not translated to proteins (Figure 1C), consistent with the observation that perplexed researchers in the past studies[8]. lncRNAs and transposons were more abundantly transcribed in spermatocytes than testis somatic epithelia (Figure 1D, E)[1-4]. Moreover, RNA fluorescence *in situ* hybridization (FISH) revealed marked upregulation of various satellite DNA transcription in spermatocytes, which cannot be captured by RNA sequencing that only identified polyadelynated RNAs[1] (Figure 1F, S1). Most of satellite DNA found in *Drosophila melanogaster* genome[14,19-21] were found to be transcribed in spermatocytes, with many of them exhibiting the signal from both strands (Figure 1F, S1).

A known source of satellite transcripts is satellite DNA embedded in the gigantic introns of several Y-linked genes[21-24]. However, these intronic satellite DNA from the Y-linked genes is not the sole source of satellite transcripts, because the large amount of satellite transcripts remained in the spermatocytes from X/O males that lack the Y chromosome (Figure 1G, S1). Satellite transcripts in X/O males are likely from pericentromeric regions of X and autosomal chromosomes, where these satellite DNA sequences are mostly found[14,19]. Taken together, these results establish widespread nature of spermatocyte transcription, including protein-coding genes, non-coding RNA and satellite DNA.

HP2 regulates transcription of AAGAG satellite DNA in spermatocytes

As an initial step toward understanding the potential function of satellite DNA transcription, we searched for a regulator of satellite DNA transcription using a list of spermatocyte enriched DNA binding proteins (Method)[1]. We chose to study heterochromatin protein 2 (Su(var)2-HP2, hereafter HP2), an HP1-intearcting protein (Figure S2A)[25,26] expressed

in spermatocytes (Figure S2B, C)[1]. Analysis of HP2 ChIP-seq data on the modENCODE database[27] showed that HP2 binds preferentially to AAGAG satellite DNA (Figure 2A).

Using *hp2-gfp* driven by its endogenous promoter[28], we confirmed that HP2 is expressed in spermatocytes as well as mitotically proliferating germ cells (e.g., germline stem cells and spermatogonia) (Figure S2C). When HP2 was depleted in mitotically-proliferating germ cells using *nos-GAL4*-driven RNAi construct (*nos-GAL4>UAS-HP2*^{HMS01699}, hereafter *nos>HP2*^{RNAi}), germ cells were depleted, suggesting that HP2 is essential for their viability (Figure S2D), as was shown for other mitotically dividing cells[29]. However, HP2 depletion from late spermatogonia/spermatocytes using *bam-GAL4* driver (*bam-GAL4>UAS-HP2*^{HMS01699}, hereafter *bam>HP2*^{RNAi}) did not lead to spermatocyte death and cells were able to proceeded to meiosis and sperm differentiation, exhibiting defects only in much later stages (see below).

We found that *bam>HP2*^{RNAi} led to marked reduction of transcripts from AAGAG satellite DNA in spermatocytes: both strands of AAGAG satellite DNA (i.e., AAGAG RNA and CUCUU RNA) were reduced in *bam>HP2*^{RNAi}, with more severe reduction of AAGAG RNA (Figure 2B, C). In contrast, *bam>HP2*^{RNAi} has little effect on transcription of other satellite DNA (Figure S3), suggesting that HP2 regulates satellite DNA transcription in a sequence-specific manner. Expression of RNAi-resistant HP2 rescued transcription of AAGAG satellite DNA (both strands) in *bam>HP2*^{RNAi} (Figure S2E, F), demonstrating that reduction in AAGAG/CUCUU RNA is indeed caused by HP2 depletion.

It was previously shown that AAGAG RNA can be depleted by RNAi (*bam-GAL4>UAS-AAGAG*^{shRNA}, hereafter *bam>AAGAG*^{RNAi})[3,30]. We confirmed that *bam>AAGAG*^{RNAi} specifically depleted AAGAG RNA without affecting the opposite strand, CUCUU RNA (Figure 2B, C) as previously shown[3]. These results suggest that *bam>HP2*^{RNAi} interferes with the transcription of AAGAG satellite DNA, whereas *bam>AAGAG*^{RNAi} cleaves AAGAG RNA after it is transcribed. In conclusion, HP2 is required for the transcription of AAGAG satellite DNA.

HP2 depletion leads to subfertility

To understand the function of HP2, which may hint at the function of AAGAG transcription in spermatocytes, we examined the phenotype of *bam>HP2*^{RNAi}, comparing it to *bam>AAGAG*^{RNAi}. We found that *bam>HP2*^{RNAi} leads to reduction in fertility, whereas *bam>AAGAG*^{RNAi} led to complete sterility as shown previously[3] (Figure 3A). Majority of *bam>HP2*^{RNAi} animals still had mature sperm in their seminal vesicles, corresponding to their residual fertility, whereas *bam>AAGAG*^{RNAi} animals had no sperm in their seminal vesicles (Figure 3B).

Several lines of evidence suggest that the subfertility in *bam>HP2*^{RNAi} and sterility in *bam>AAGAG*^{RNAi} are caused by distinct mechanisms. RT-qPCR showed that *bam>AAGAG*^{RNAi} led to downregulation of a subset of Y-linked fertility genes (e.g., *ORY* and *kl-2*), whereas *bam>HP2*^{RNAi} did not affect these genes (Figure 3C). *ORY* and *kl-2* genes are known to contain large stretch of AAGAG satellite DNA in their gigantic introns (Figure S4)[21,23]. qRT-PCR with primers that are designed to amplify spliced products joining exon 4 and exon 5 in *ORY* gene, which span across AAGAG satellite-containing gigantic intron, revealed striking reduction of *ORY* transcripts in *bam>AAGAG*^{RNAi}, whereas *bam>HP2*^{RNAi} did not show any reduction in *ORY* transcripts (Figure 3D). RNA FISH further confirmed marked reduction of *ORY* mRNA in spermatocytes in *bam>AAGAG*^{RNAi} animals, but not in *bam>HP2*^{RNAi} animals (Figure 3E). *Pzl* is an autosomal gene that contains gigantic introns with assembly gaps[31], and careful inspection of sequences near assembly gaps in *Pzl* revealed the presence of intronic AAGAG satellite DNA (Figure S4). RT-qPCR showed that *Pzl* is also downregulated in *bam>AAGAG*^{RNAi} but not in *bam>HP2*^{RNAi} (Figure 3C). These results suggest that *bam>AAGAG*^{RNAi} leads to cleavage of AAGAG-containing RNA. Because *ORY* and *kl-2* are required for male fertility, we speculate that the sterility of *bam>AAGAG*^{RNAi} is caused by RNAi-mediated knockdown of these genes that contain AAGAG in their introns.

In contrast, *bam>HP2*^{RNAi} does not lead to downregulation of these fertility genes, suggesting that *bam>HP2*^{RNAi} impacts spermatogenesis through a mechanism distinct from *bam>AAGAG*^{RNAi}. Based on proper expression of *ORY* and *kl-2* genes that contain AAGAG satellite DNA in their introns, we infer that these genes' intronic AAGAG is properly expressed in *bam>HP2*^{RNAi}[24]. Indeed, the residual transcription of AAGAG/CUCUU was observed in *bam>HP2*^{RNAi} spermatocytes, which may represent intronic satellite transcripts (Figure 2B). These results imply that the reduced fertility of *bam>HP2*^{RNAi} animals is not due to downregulation of Y-linked fertility factors.

HP2 depletion leads to defective histone-to-protamine transition in spermatids

The above results suggest that subfertility caused by HP2 depletion is not due to defective expression of Y-linked fertility genes. To further determine the cause of subfertility of *bam>HP2*^{RNAi} animals, we explored the possible defects during spermatogenesis in *bam>HP2*^{RNAi}. Upon HP2 depletion, spermatocytes appeared to develop normally (other than reduced satellite RNA), and they underwent apparently normal meiosis (Figure S5), suggesting that defects occur in post-meiotic stages. Indeed, we found that *bam>HP2*^{RNAi} led to unique cytological phenotype during spermatid differentiation stage. In wild type animals, post-meiotic

germ cells undergo stereotypical morphological changes, leading to the formation of mature sperm: a cyst of 64 spermatids, resulting from 4 mitotic and 2 meiotic divisions, develop in synchrony to undergo sperm DNA compaction and axoneme elongation (Figure 1A). Compaction of sperm DNA is mediated by replacement of histone-based chromatin with protamine-based chromatin (Figure 4A)[15,16]. We found that *bam>HP2*^{RNAi} led to defective sperm DNA compaction during the last stages of sperm development (Figure 4B): In some cases (Figure 4B, ii), a subset of spermatid nuclei within a cyst lost their typical 'needle' morphology (Figure 4B, i) and become completely rounded-up, while other nuclei exhibited normal needle morphology. In other cases, all spermatids within a cyst (Figure 4B, iii) exhibited defective sperm nuclear morphology. Expression of RNAi-resistant HP2 rescued sperm DNA compaction defect in *bam>HP2*^{RNAi} (Figure 4B, iv), demonstrating that sperm DNA compaction defect is indeed due to HP2 depletion.

Although the morphology of earlier 'canoe' stage spermatids appeared mostly normal in *bam>HP2*^{RNAi} animals, we found that the defects begin in these earlier stages. Canoe stage spermatid is characterized by removal of histone and incorporation of protamine, such as Mst77F (Figure 4C, control)[15]. In control animals, sperm DNA compaction was accompanied by sequential events of removing heterochromatin mark H3K9me3, removing histone H3.3 (Figure S6), then incorporating protamine such as Mst77F (Figure 4C). However, in *bam>HP2*^{RNAi} animals, a subset of spermatids exhibited a failure in the removal of H3K9me3 and deposition of Mst77F, whereas other nuclei in the same cyst have removed H3K9me3 and deposited Mst77F (Figure 4C). Moreover, when the cyst progressed to the needle spermatid stage, the defective nuclei in *bam>HP2*^{RNAi} that failed to compact their DNA still retained H3K9me3 (Figure 4D). Taken together, these results suggest that retention of H3K9me3 underlies failure in protamine incorporation, leading to ultimate failure in sperm DNA compaction, in *bam>HP2*^{RNAi}.

HP2 depletion preferentially impacts Y-chromosome containing spermatids

How does *bam>HP2*^{RNAi} lead to failure in sperm DNA compaction? It is possible that HP2 regulates expression of many genes through its ability to control heterochromatin. Alternatively, the phenotype of *bam>HP2*^{RNAi} may be explained by the loss of AAGAG transcription.

Insight into these questions was obtained unexpectedly. While counting the number of offspring for the fertility assay (Figure 3A), we noticed that *bam>HP2*^{RNAi} males produce significantly more daughters than sons (Figure 5A), suggesting that sperm DNA compaction defects may be biased toward Y chromosome-containing spermatids. Indeed, by DNA FISH

using X- and Y-specific probes, we found that defective nuclei in *bam>HP2*^{RNAi} predominantly contained the Y chromosome (Figure 5B), demonstrating that the Y chromosome is more sensitive to HP2 depletion than the X chromosome. Interestingly, the Y chromosome contains much more AAGAG satellite DNA than the X chromosome[14,19] (Figure 5C). Based on this correlation between the amount of AAGAG on the chromosome and the tendency to fail in sperm DNA compaction, we hypothesized that HP2-dependent transcription of AAGAG satellite DNA facilitates remodeling of its heterochromatin state in preparation of histone-to-protamine transition (Figure 5D): That is, the chromosomes with more AAGAG satellite DNA are more dependent on HP2 for its transcription-dependent heterochromatin remodeling. Accordingly, the chromosomes with less AAGAG satellite DNA may be more resistant to the loss of HP2 because their chromatin remodeling is not dependent on HP2. This can explain why X chromosome-containing spermatids are less impacted by HP2 depletion, because X chromosome has less AAGAG satellite DNA. The fact that *bam>HP2*^{RNAi} impacts Y chromosome-containing spermatids more than X-containing ones suggests that the defects are not caused by gene expression changes due to *bam>HP2*^{RNAi}, which would impact all spermatids without chromosome-specific bias.

Chromosome II with minimal amount of AAGAG satellite DNA is more resistant to HP2 depletion

According to the model presented above, any chromosome with AAGAG satellite DNA would be sensitive to HP2 depletion. Chromosome II contains considerable amount of AAGAG in its pericentromeric heterochromatin (Figure 5C)[14,19], likely contributing to spermatid DNA compaction defects in *bam>HP2*^{RNAi}. This may also explain why sometimes all spermatids within a cyst (Y-containing as well as X-containing spermatids within a cyst) fail to undergo sperm DNA compaction defects (Figure 4B, iii).

To test the possibility that the defect in sperm DNA compaction in *bam>HP2*^{RNAi} is caused by abundance AAGAG satellite DNA (Figure 5D), we took advantage of a natural chromosome II variant with minimal AAGAG satellite DNA (hereafter II$^{\Delta AAGAG}$)[32] (Figure S7). When this chromosome II$^{\Delta AAGAG}$ was placed in the background of *bam>HP2*^{RNAi} (*y*$^{+}$*w*$^{+}$*/Y; P{y*$^{+}$*=UAS-HP2*^{HMS01699}*}2/ΔAAGAG; P{w*$^{+}$*=bam-GAL4}3/+,* hereafter X/Y; II^{+}/II$^{\Delta AAGAG}$ (*bam>HP2*^{RNAi})), we observed a considerable reduction in the frequency of defective spermatids that failed sperm DNA compaction (Figure 6A, B). Taken together, these results suggest that the abundance of AAGAG satellite DNA correlates with the severity of sperm DNA compaction defects due to HP2 depletion.

To further test our hypothesis that AAGAG satellite DNA amount determines the sensitivity of spermatids to HP2 depletion, we examined whether spermatids containing $II^{\Delta AAGAG}$ survived better than those with II^{+} in *bam>HP2*^{RNAi}. Specifically, we analyzed the genotype of the offspring of X/Y; $II^{+}/II^{\Delta AAGAG}$ (*bam>HP2*^{RNAi}). From diploid X/Y; $II^{+}/II^{\Delta AAGAG}$ spermatocytes, there are four possible genotypes of the haploid sperm: X II^{+}, X $II^{\Delta AAGAG}$, Y II^{+}, and Y $II^{\Delta AAGAG}$ (Figure 6C). Based on the offspring genotype, we deduced the genotype of survived sperm. In male offspring, where II^{+} and $II^{\Delta AAGAG}$ can easily be scored based on the body color (Method), we observed a small but significant overrepresentation of $II^{\Delta AAGAG}$ over II^{+} (Figure 6D), suggesting that spermatid containing Y $II^{\Delta AAGAG}$ indeed survived better than Y II^{+}. This implies that AAGAG satellite DNA on chromosome II worsens sperm DNA compaction defects in Y-containing spermatids.

In female offspring, II^{+} and $II^{\Delta AAGAG}$ cannot be easily distinguished by visible phenotypic markers. Thus, a subset of randomly-chosen female offspring was subjected to PCR-based assay to distinguish between II^{+} and $II^{\Delta AAGAG}$ (Method), which showed no significant difference in the survival of X II^{+} and X $II^{\Delta AAGAG}$ (Figure 6D). Although this may be due to a limited number of sample size, it may reflect the dose-sensitive nature where HP2-depleted cells can tolerate only a certain amount of AAGAG satellite DNA: X-containing spermatids may be able to tolerate AAGAG satellite DNA on the chromosome II, because they contain only a small amount of AAGAG satellite DNA on the X chromosome. In contrast, Y-containing spermatids, which carries a large amount of AAGAG satellite DNA, cannot tolerate AAGAG satellite DNA on the chromosome II under HP2 depletion. Accordingly, sperm DNA compaction defects of Y-containing spermatids in *bam>HP2*^{RNAi} can be rescued by reducing the dose of AAGAG satellite DNA on the chromosome II.

Taken together, these results suggest that the abundance of AAGAG satellite DNA is a determinant that renders spermatid sensitive to the loss of HP2. The fact that the reduction of AAGAG satellite DNA markedly rescues the phenotype of *bam>HP2*^{RNAi} implies that AAGAG satellite DNA is the major target of HP2, although HP2 may also regulate other heterochromatic loci as well. Additionally, the rescue of the phenotype by the reduction of AAGAG satellite DNA amount implies that AAGAG transcripts are not essential for spermatid development. We propose that HP2 promotes transcription of AAGAG satellite DNA in spermatocyte, facilitating the remodeling of heterochromatin in preparation of germline DNA for histone-to-protamine transition.

DISCUSSION

Functional significance of widespread transcription in the testis has been enigmatic. Several hypotheses have been put forward to explain the puzzling transcriptomic profile of the testis that includes the transcription of noncoding DNA as well as transcription of protein coding genes without translation. Here, through the study of satellite DNA transcription in *Drosophila* spermatocytes, we propose that the widespread transcription in male germline reflects the process of chromatin remodeling in preparation for histone-to-protamine transition. We showed that satellite DNA is abundantly transcribed in *Drosophila* spermatocytes, where widespread transcription occurs. We identified HP2 as a transcriptional regulator of AAGAG satellite DNA in spermatocytes. In the absence of HP2 in spermatocytes (*bam>HP2*^{RNAi}), AAGAG transcription was diminished, which was accompanied by retention of heterochromatin marks. We propose that the lack of chromatin remodeling, particularly that of heterochromatin, interfere with the process of histone-to-protamine transition, leading to sperm DNA compaction defects. Strikingly, we found that spermatids with more AAGAG satellite DNA are more likely to die under *bam>HP2*^{RNAi}. Based on these results, we propose that HP2-mediated AAGAG satellite DNA transcription in spermatocytes reorganizes heterochromatin for protamine incorporation in spermatids.

According to this model, it is transcription, but not transcripts, that is important for male germ cell development. Although it is challenging to distinguish between the function of transcription to remodel the chromatin and that to generate functional transcripts, several lines of evidence favor the model that transcription, but not resultant transcripts, is more important. First, *bam>AAGAG*^{RNAi}, which diminishes AAGAG transcripts, did not lead to the sperm DNA compaction defect phenotype similar to *bam>HP2*^{RNAi}. Instead, it led to sterility due to depletion of Y-linked genes that contain AAGAG satellite DNA in their gigantic introns (most strikingly the *Ory* gene). Second, if AAGAG transcripts have any function, it would be expected that deletion of AAGAG satellite DNA in II$^{\Delta AAGAG}$ worsens the phenotype of *bam>HP2*^{RNAi} because both reduce AAGAG transcripts. Instead, II$^{\Delta AAGAG}$ rescued *bam>HP2*^{RNAi} phenotype, implying that AAGAG RNA is dispensable for spermatid development. Rather, the results imply that AAGAG satellite DNA is a ‘burden’ for spermatid development, whose heterochromatic nature impedes sperm DNA compaction unless remodeled by HP2-mediated transcription. Finally, although it possible that the phenotype of *bam>HP2*^{RNAi} could be caused by HP2’s other targets than AAGAG satellite DNA, rescue of the *bam>HP2*^{RNAi} phenotype by deletion of AAGAG satellite DNA in II$^{\Delta AAGAG}$ indicates that the major contributor to explain the *bam>HP2*^{RNAi} phenotype is AAGAG satellite DNA.

HP2-mediated transcription of AAGAG satellite DNA likely represents just one example of many transcription regulators in testis reorganizing chromatin for protamine incorporation. Among many heterochromatic satellite DNA blocks in *Drosophila* genome, HP2 appears to regulate mainly the transcription of AAGAG, whereas other satellite DNA such as AACATAGAAT, AATAT, AACAC, and AAGAC were not detectably impacted. Therefore, we speculate that there are other factors that serve the same function as HP2 but for different satellite DNA. By extending this model, we further propose that the widespread transcription of the testis is the result of the process that remodels germ cell chromatin to allow histone-to-protamine transition. We predict that a panel of transcription factors (to express satellite DNA, noncoding RNA, genic DNA) together contribute to transcription of a large fraction of the genome in male germline. Discovery of such factors awaits future investigations.

In summary, the present study provides a model to explain the significance of widespread transcription broadly observed in male germline, where it serves to remodel the chromatin of male germline to make it compatible with histone-to-protamine transition.

Limitations of the study

This study proposes that widespread transcription of male germ cells is the results of chromatin remodeling to prepare for the process of histone-to-protamine transition. This model implies that it is transcription but not transcripts per se that is important for male germ cell development. However, our study still leaves the possibility that transcripts also serve functions, for example serving as a precursor of piRNA that regulates their chromatin status[33]. Additionally, causal relationship between transcription and chromatin remodeling cannot be fully established, because it is impossible to separate these two (e.g., transcription without remodeling).

Acknowledgements: We thank Dr. Gary Karpen, and Dr. Andrew Clark for reagents, and the members of the Yamashita lab for discussions and comments on the manuscript. We thank the FlyBase, Bloomington *Drosophila* Stock Center, and *Drosophila* Genomics Resource Center for reagents and information. **Funding:** This research is funded by the Howard Hughes Medical Institute and Whitehead Institute for Biomedical Research (to Y.M.Y). **Author Contributions:** Conceptualization, T.K. and Y.M.Y.; methodology, T.K.; investigation, T.K.; software, A.R.; resources, J.M.F. and Y.M.Y.; writing – original draft, T.K.; writing – editing, T.K. and Y.M.Y.; funding acquisition, Y.M.Y.; supervision, Y.M.Y. **Competing Interests:** The authors declare no competing interests. **Data and materials availability:** All study data are included in the article.

Materials and Methods

Fly Husbandry

All experimental flies were raised on modified Bloomington *Drosophila* Stock Center (BDSC) cornmeal food (agar 0.65%, cornmeal 6.71%, inactivated yeast 1.59%, soy flour 0.92%, corn syrup 7.0%, tegosept 0.15%; without propionic acid; less dry time) at 25°C, and young flies (1- to 3-day-old adults) were used for all experiments. All fly stocks were maintained at room temperature while not in use for experiments, and stocks that exhibited spontaneous spermatid DNA compaction errors were replaced with new stocks. Control flies were either the sibling from the same genetic cross or the parental *GAL4* stock. The following fly stocks were used: y^1w^1 (BDSC 1495), *nos-GAL4:VP16*[34], $P\{w^{+mC}$*=bam-GAL4:VP16}3*[35], $P\{w^{+}$*=Ub-GFPS65C:α1-tub84B}1*[36], *H3.3A-Dendra2*[37], *C(1)RM/C(1;Y)6,* $y^1w^1f^1/O$ (BDSC 9460; males from this stock were crossed with y^1w^1 females to generate X/O males), $P\{y^{+t7.7}v^{+t1.8}$*=TRiP.HMS01699}attP40* (BDSC 38255; *UAS-HP2*^{RNAi}), *UAS-AAGAG*^{shRNA} (gift from Gary Karpen[3]), *Pbac{*$y^{+mDint2}w^{+mC}$*=Su(var)2-HP2-GFP.FPTB}VK00033* (BDSC 68184; *hp2-gfp*), *UAS-HP2-S* (this study), *UAS-HP2-L* (this study), Ithaca I16 and Beijing B52 of Global Diversity lines (gift from Andrew Clark[32]). Combinations of transgenes were generated using the CyO; TM6B double balancer strain.

Immunofluorescence (IF) Staining

Testes were dissected in 1X PBS, and fixed for 30 minutes at room temperature (RT) in 1mL fixative (1X PBS (Invitrogen AM9624; 4mL of 10X PBS), 4% formaldehyde (ThermoFisher Scientific 28908; 10mL of 16% solution), 0.1% Triton X-100 (Millipore Sigma T9284; 400μL of 10% solution) in H_2O (25.6mL); stored at −20˚C). Testes were rinsed with 1mL PBST (1X PBS (Invitrogen AM9624; 5mL of 10X PBS), 0.1% Triton X-100 (Millipore Sigma T9284; 500μL of 10% solution) in H_2O (44.5mL); stored at 4˚C), permeabilized for at least 3 hours at RT in 1mL PBST, blocked for 1 hour at RT in 200μL blocking solution (1X PBS (Invitrogen AM9624; 5mL of 10X PBS), 3% BSA (Fisher Scientific BP1605-100; 1.5g in 25mL H_2O), 0.1% Triton X-100 (Millipore Sigma T9284; 500μL of 10% solution) in H_2O (up to 50mL); stored at −20˚C), and incubated overnight at 4°C in 200μL blocking solution with primary antibodies. Samples were rinsed with 1mL PBST, washed for at least 1 hour at RT in 1mL PBST, incubated overnight at 4°C in 200μL blocking solution with secondary antibodies, rinsed and washed as above. Samples were mounted in VECTASHIELD with DAPI (Vector Laboratories H-1200). Images were acquired using Leica Stellaris8 confocal microscope with a 63X oil immersion objective lens (NA = 1.4) and processed/analyzed using ImageJ software. The primary antibodies used

were anti-Mst77F (1:1000 dilution; guinea pig; Yamashita lab[38]) and anti-H3K9me3 (1:200 dilution; rabbit; Abcam ab8898). The secondary antibodies used were anti-rabbit IgG conjugated with Alexa Fluor 647 (1:200 dilution; goat; Abcam ab150079) and anti-guinea pig IgG conjugated with Alexa Fluor 568 (1:200 dilution; goat; Abcam ab175714).

RNA Fluorescent *in situ* Hybridization (FISH)

Testes were dissected in 1X PBS, and fixed for 30 minutes at RT in 1mL fixative. Testes were washed briefly (5 min x 2) at RT in 1mL PBST, rinsed briefly (5 min) at RT with 1mL wash buffer (2X SSC (Invitrogen AM9770; 5mL of 20X SSC), 10% formamide (Millipore Sigma S4117; 5mL), 0.1% Triton X-100 (Millipore Sigma T9284; 500µL of 10% solution) in H_2O (39.5mL); stored at 4˚C), and hybridized overnight at 37°C in 200µL hybridization buffer (10% dextran sulfate (Millipore Sigma D8906; 1g in 5mL H_2O), 1mg/mL yeast tRNA (Millipore Sigma R8759; 1mL of 10mg/mL solution), 0.5% BSA (Invitrogen AM2616; 1mL), 2X SSC (Invitrogen AM9770; 1mL of 20X SSC), 10% formamide (Millipore Sigma S4117; 1mL), 2mM Ribonucleoside Vanadyl Complex (NEB S1402; 100µL) in H_2O (up to 10mL); stored at −20˚C). Following hybridization, samples were washed two times in wash buffer for 30 minutes each at 37°C and mounted in VECTASHIELD with DAPI (Vector Laboratories H-1200). Images were acquired using Leica Stellaris8 confocal microscope with a 63X oil immersion objective lens (NA = 1.4) and processed/analyzed using ImageJ software. RNA FISH signal intensity is semi-quantitative due to inherent technical (e.g., different tubes) and biological (e.g., testis thickness) variations. RNA FISH intensities among different genotypes (Figure 2C) were analyzed from images with roughly the same intensity of internal control (GFP-tubulin). Fluorescently labeled probes were added to the hybridization buffer to a final concentration of 50nM (1µL of 10µM probe solution in 200µL hybridization buffer). Probes against the repetitive DNA transcripts were from Integrated DNA Technologies: Cy5-(AAGAG)x6, Cy3-(CTCTT)x6; Cy3-(AATAACATAG)x3, Cy5-(CTATGTTATT)x3; Cy5-(AATAT)x6, Cy3-(ATATT)x6; Cy3-(AACAC)x6, Cy5-(GTGTT)x6; Cy3-(AAGAC)x6, Cy5-(GTCTT)x6. *ORY* probes Quasar 670-(TTTTTGGCTTTCTTTCTGTC, AAAAGTTGAGGCTCCGAGTT, CGTTTAATTCGCGATGCTTC, CTTCATCTACATACCGACGA, TCCGATGTTGAAGTCAGTTC, CCCCCAACAAATCTTTAAGT, TGATGCATCTGATTCTTTCC, TCTTGCACTAACTGTTCTCG, CAGTTGTACCACTATTTCGG, TTAGCTCGAGAAGCCATTTT, ATTCAACGTTTAGGCGTTCG, CCATTGTCTTCATCAAAGCT, TTTCCATGTGCTTCTTTTTG, CTCTATTCGCAATATCCAGT, AGTTTACGTGTCGTTTCTGA, GCATTGCCTTATTTAATGCG, GCCTTAACTGCTTTATCATT, AAGCCTGCTCGTTAATTGAG, TTGTACATTCTTGTTGTCGC, CATCCTTCTCCAGAGAATTA, GACGAATATCATCCGTTCGG,

CACGTTGCAATGTCTCTTTG, ATGTTTTAAGTCCGCCATAG, TCTTTCTCTGCTTTGGATTT, CGTCTTCAGAGAGATTTGGT, TCGTGTAACTTTTCCGTGAG, ACGGACTCCAACTGTTTTTT, CGCTGAAGCATCATTTTCTC, TTTTACTTCGTTTGCGCTTA, GCCACTAAGTTTTCTTTGTT, TTTCTCTCATATCCTTACGT, CAATCCGACTAGGTTACGTT, AACAATCTCGTCATTCCGTC, GGGCATTTTGTGCAATTTGA, AAGGCATTCACTTTCAGTGT, CTCATGTCAGCAGTACTTTT, TCTTCAGTTAGAGCTCGTAT, CAACGATGTACTCCTGTAGG, AATTTCTTAGGATCTTCGCC, TATTGACTGCTTTAGGGAGC, AGCCTCACACAGTTTATTTT, GCATATGAGATAGCATCCTT, TAATGAACGCTCTGCTGCTA, GTCTTGATTTAAGTTCCACC, AATTGACAGCTCTCCGATTT, TATTTCGTTTTTCCCATCTG, ATCCACATTCCATATACTCT, ATATCCGTTAACTTCGCACA)

Reverse Transcribed Quantitative Polymerase Chain Reaction (RT-qPCR)

Dissected testes from 50 flies were pooled in ice-cold 1mL 1X PBS. Samples were first homogenized in ice-cold 300μL TRIzol (Invitrogen 15596026), supplemented with 700μL TRIzol, vortexed vigorously, centrifuged for 5 min at 4˚C. Approximately 1mL of clear supernatant was transferred to a new tube, and 400μL of phenol:chloroform (Invitrogen AM9722) was added. Samples were mixed gently by hand for 15 sec, incubated for 3 min at RT, centrifuged for 15 min at 4˚C. Approximately 400μL of the top aqueous phase was transferred to a new tube, and 1μL of GlycoBlue Coprecipitant (Invitrogen AM9515), 1mL of 100% ethanol, and 140μL of 5M NH_4Oac were added. RNA samples were stored at −80˚C until the RT reaction. RNA samples were centrifuged for 20 min at 4˚C (discard supernatant), washed with 700μL 70% ethanol, centrifuged for 10 min at 4˚C (discard supernatant), dried for 15 min at RT, and dissolved in 20μL of 95˚C H_2O. RNA was denatured for 5 min at 65˚C and put on ice at least for 1 min. Almost all RNA (20μL, typically 5μg RNA yield) was used for synthesis of cDNA (mixed with 25μL buffer and 5μL SuperScript III (Invitrogen 11752); 25˚C 10min, 50˚C 30min, 85˚C 5min, 4˚C keep; stored at −20˚C). Quantitative PCR was done using PowerUp SYBR Green Master Mix (Applied Biosystems A25742; 10μL reaction volume with 5μL of 2X PowerUp SYBR Green Master Mix, 3.5μL H_2O, 0.5μL cDNA, and 1μL of 5μM forward and reverse primer mix; Primers from IDT were dissolved with H_2O to make 100μM stock, and 10μL of 100μM forward primer and 10μL of 100μM reverse primer were mixed with 180μL H_2O to make 5μM primer mix) and assessed with QuantStudio 6 Flex system (Applied Biosystems; 96-well, 0.2mL; standard curve; SYBR Green reagents; standard) with the following PCR condition: 50˚C 2 min, 95˚C 2 min; 40 cycles of 95˚C 15s, 55˚C 15s, 72˚C 60s (PCR Stage); continuous cycles of 95˚C 15s, 55˚C 15s, 95˚C 15s (Melt Curve Stage). Expression values calculated from the $2^{-\Delta\Delta Ct}$ comparative Ct method, $2^{\wedge-\{(Ct^{Target,\ Experimental} - Ct^{Housekeeping,\ Experimental}) - (Ct^{Target,\ Control} - Ct^{Housekeeping,\ Control})\}}$.

Primers used for this study are as follows: HP2-S Fwd 5'-ATTTGGGTGACTTATACGGGGACT-3', HP2-L Fwd 5'-ATCCCGAACCCAGCACAT-3', HP2 Rev 5'-CTGGTTTAACTTGTTCCTTTTTGCCAGT-3', Und (as housekeeping) Fwd 5'-GCAAGAAAAGCGGTCAGACT-3', Und (as housekeeping) Rev 5'-CGTGTTGATACGGTCCAGAG-3', kl-5 Fwd 5'-TGTCTATGAGTGCCCAGTTTAC-3', kl-5 Rev 5'-GTCCACTTACTTGCTCTCTCTC-3', kl-3 Fwd 5'-ATGGTGCTGGTTGGGATAAG-3', kl-3 Rev 5'-TTGGCAGCCGTTGAGAAT-3', kl-2 Fwd 5'-TTTACCAGTGTCCCGCATATT-3', kl-2 Rev 5'-AGTGCAGTACCTCGCTTTATC-3', ORY (Last Exon) Fwd 5'-CAGCGTATAAACCGACAAATGG-3', ORY (Last Exon) Rev 5'-GACAGCTCTCCGATTTCACTAA-3', ORY (Exons 4-5) Fwd 5'-ACTGTGCACTTCCCTTTGT-3', ORY (Exons 4-5) Rev 5'-GAGATGAAATGGCGCAAGAAAT-3', CCY Fwd 5'-CGGAGCCGTAAAGGATGATT-3', CCY Rev 5'-CGCTGACCTGATAACCCTATTC-3', DIP-λ Fwd 5'-ACACCCTGGATACTCACAAATG-3', DIP-λ Rev 5'-AGTGAAACACACGCCAGAA-3', CG44666 Fwd 5'-GCCGATTTGTGCAGTCTTTC-3', CG44666 Rev 5'-GGACGATGTGGATGCTGTTA-3', Myo81F Fwd 5'-CCTCTTCATCGAGCGACTATTT-3', Myo81F Rev 5'-ACGATGTTCCAGTAGGTGAATAC-3', Pzl Fwd 5'-GGATGATATCCTACTACCAGCTTTG-3', Pzl Rev 5'-CCGGATAACAAGCCTCCTTTAT-3', Mitf Fwd 5'-TCAGATGACTGTTGCGGTATAA-3', Mitf Rev 5'-ATACCCGTGTGGTGAGAATG-3'.

DNA FISH

Adult testes (for meiotic chromosome spread, typically three flies per slide) or third instar larval brains (for mitotic chromosome spread, typically three larvae per slide) were dissected in PBS. Samples were fixed for 4 min at RT in 50 µL of modified fixative (45% acetic acid (450µL of glacial acetic acid) and 2.5% formaldehyde (550µL of fixative described earlier)) placed on Superfrost Plus microscope slides (ThermoFisher Scientific 22-037-246). Samples were squashed under a coverslip, and then immediately frozen in liquid nitrogen. Coverslips were quickly removed and slides were immediately dehydrated in a Coplin jar filled with 100% ethanol. Then, slides were dried at RT at least for 1 hour. 17 µL of hybridization buffer (10% dextran sulfate (Millipore Sigma D8906; 1g in 2mL H_2O), 50% formamide (Millipore Sigma S4117; 5mL), 2X SSC (Invitrogen AM9770; 1mL of 20X SSC), 10mM EDTA (Invitrogen AM9260G; 200µL of 0.5M EDTA) in H_2O (up to 8.5mL); stored at −20˚C) was mixed with 3µL probe mix (0.5 µM probe (1µL of 10µM probe solution) up to three colors or substitute with H_2O). This hybridization mix was applied to samples on a slide and covered with a cover slip. Samples were incubated at 95°C for 5 min, cooled and wrapped in parafilm, then incubated

overnight at RT in a dark humid chamber. In a Coplin jar filled with 0.1X SSC (5mL of 20X SSC diluted with H_2O up to 1L), coverslips were removed and slides were washed three times for 15 min each. Slides were dried, sample locations were marked, and samples were mounted in VECTASHIELD with DAPI (Vector Laboratories H-1200). For the whole testis staining, testes were dissected in 1X PBS, fixed for 30 minutes at RT in 1mL modified fixative (1mM EDTA (Invitrogen AM9260G; 2μL of 0.5M EDTA) and 1mL of fixative described earlier), rinsed with 1mL PBST-EDTA (1X PBS (Invitrogen AM9624; 5mL of 10X PBS), 0.1% Triton X-100 (Millipore Sigma T9284; 500μL of 10% solution), 1mM EDTA (Invitrogen AM9260G; 100μL of 0.5M EDTA) in H_2O (44.4mL); stored at RT), washed for 1hr at RT in 1mL PBST-EDTA, rinsed with 1mL PBST (no EDTA), incubated for 10 min at 37˚C in 100μL RNase A (2mg/mL in PBST), washed for 10 min at RT in 1mL PBST-EDTA, rinsed with 1mL SCCT-EDTA (50mL SCCT (5mL of 20X SSC and 250μL of 20% Tween in 45mL H_2O; stored at RT) and 100μL of 0.5M EDTA; stored at RT), washed for 15 min at RT in 100μL SCCT-20%F (800μL SCCT and 200μL formamide, freshly made), washed for 15 min at RT in 100μL SCCT-40%F (600μL SCCT and 400μL formamide, freshly made), washed for 15 min at RT in 100μL SCCT-50%F (500μL SCCT and 500μL formamide, freshly made), washed for 30 min at RT in 100μL SCCT-50%F, and put in 100μL hybridization mix (85μL hybridization buffer mixed with 5μL of 10μM probe up to three colors or substitute with H_2O). Samples were denatured for 5 min at 95˚C and hybridized overnight at 37˚C. Following hybridization, samples were washed two times in 1mL SCCT-EDTA for 30 minutes each at RT and mounted in VECTASHIELD with DAPI (Vector Laboratories H-1200). Images were acquired using Leica Stellaris8 confocal microscope with a 63X oil immersion objective lens (NA = 1.4) and processed/analyzed using ImageJ software. Probes used for this study are as follows: Cy3-(TAGA)x8, Cy3/Cy5-(AATAC)x6, Cy5/AF488-(AAGAG)x6.

Genotyping

X/Y; II+/II$^{\Delta AAGAG}$ (*bam>HP2^{RNAi}*) were mated with *y^{1}w^1* females for 5 days, and the eclosed flies was collected a week later for genotyping. The *y*$^+$ transgene on II$^+$ was used to genotype male offspring by the *y*$^+$ body color. Because X/Y; II$^+$/II$^{\Delta AAGAG}$ (*bam>HP2^{RNAi}*) carry a wild-type X chromosome with the endogenous *y*$^+$ gene, female offspring was genotyped by PCR using *y*$^+$ transgene-specific sequences. Each fly was homogenized in 50μL extraction buffer (1X TE (Sigma Aldrich 93283; 49μL), 25mM NaCl (0.5μL of 2.5M NaCl), 200μg/mL proteinase K (0.5μL of 20mg/μL), incubated for 30 min at 37˚C followed by 1 min at 95˚C. Genomic DNA was stored in −20˚C. 1μL of genomic DNA was added in PCR mixture (DreamTaq DNA Polymerase

(ThermoFisher Scientific EP0705; 0.2μL), 0.5μM primer (2μL of 5μM forward and reverse primer mix), 200μM dNTP (0.4μL of 10mM dNTP), DreamTaq Green Buffer (ThermoFisher Scientific B71; 2μL) in H_2O (14.4μL)). Target is amplified by touchdown PCR (95˚C 3 min; 15 cycles of 95˚C 30s, 70˚C (−1˚C/cycle) 45s, 72˚C 30s; 20 cycles of 95˚C 30s, 55˚C 45s, 72˚C 30s; 72˚C 5 min and 10˚C keep). 10μL of PCR reaction was analyzed by gel electrophoresis of 1.5% TAE gel 120V for 45min with 2μL of 100bp ladder. Primers used for this study are as follows: Fwd 5'-CTAGAGTAAGTAGTTCGCCAGTTAAT-3' and Rev 5'-GCTGAATGAAGCCATACCAAAC-3'.

Fertility Assay

Virgin y^1w^1 females were collected 1-3 days before setting up the fly cross. Freshly prepared fly food was placed in the 25˚C incubator a day before setting up the fly cross. One male (control or *bam>HP2*^{RNAi}) and three y^1w^1 virgin females are mated for 4 days in the 25˚C incubator. Vials were placed alternately to let in the light and encourage mating. After 4 days, parents were discarded and the number of eclosed flies is counted a week later.

Transgenic Fly Generation

The codon-modified fragment of HP2 (RNAi target sequence CAGGAGAGGAATGAAGAACAA was changed to CAAGAACGCAACGAGGAGCAG) was synthesized by the IDT gBlocks Gene Fragments service (1000ng; suspended in 100μL TE to make 10ng/μL solution and incubated at 50˚C for 20 minutes; stored at −20˚C) and cloned into UFO12514 (pUAST-based vector with HP2-S cDNA, obtained from *Drosophila* Genomics Resource Center (DGRC) Stock 1648698) using In-Fusion cloning. Briefly, 0.5μL vector (at least 50ng), 0.5μL insert (at least a few fold excess of insert), 3μL H_2O, and 1μL In-Fusion Snap Assembly Master Mix (Takara Bio 638947) were mixed and incubated for 15 min at 50˚C followed by 4˚C keep; 50μL DH5α (NEB C2987) and 5μL In-Fusion reaction mixture was mixed and incubated for 15 min on ice, and the bacteria was heat shocked for 45 sec at 42˚C, on ice for 1 min, recovered in 200μL SOC (briefly if ampicillin resistant, 1h at 37˚C if non-ampicillin resistant), and cultured on a LB plate with 100μg/mL carbenicillin or other antibiotics overnight at 37˚C; Each colony is dissolved in 10μL H_2O, and 1μL was used for colony PCR (mixed with19μL DreamTaq PCR mixture used for genotyping followed by touchdown PCR that amplify the insert) and 9μL was added in 200μL LB (stored at 4˚C during colony PCR, and cultured in 3mL LB overnight at 37˚C); 500μL of cultured *E. coli* was mixed with 500μL of 50% glycerol and stored at −80˚C, and the rest of cultured *E. coli* was used to collect plasmids using Miniprep (QIAGEN 27104); The entire plasmid was sequenced by Plasmidsaurus Inc; Small cloning errors were corrected by QuikChange Lightning

Site-Directed Mutagenesis Kit (Agilent 210518). HP2-L fragments were amplified from testis cDNA library: Briefly, 1μL of cDNA and 5μL of 5μM forward and reverse primer mix for each fragment were added in PCR mixture (Herculase II Fusion DNA Polymerase (Agilent 600675; 1μL), 250μM dNTP (1.25μL of 10mM dNTP), 5x Buffer (10μL) in H_2O (31.75μL)). For each fragment, two tubes with 50μL PCR reaction were prepared and amplified by touchdown PCR, adjusting the extension time (30s/kb). The PCR products were run on 0.7% TAE gel and extracted by gel purification (QIAGEN 28506). The two HP2-L fragments were fused by overlap extension PCR: Briefly, 20μL PCR reaction (0.5μL of Herculase II Fusion DNA Polymerase, 0.5μL of 10mM dNTP, 4μL of 5x Buffer, ([length of fragment (bp) ÷ 10] ng of each fragment with H_2O) was incubated in a thermocycler (95˚C 3 min; 14 cycles of 95˚C 30s, 72˚C (−0.5˚C/cycle) 45s, 72˚C 30s/kb; 72˚C 5 min and 10˚C keep). 30μL spike-in mixture (17.75μL H_2O, 5μL of 5μM forward and reverse primer mix for the entire fragment, 6μL of 5x Buffer, 0.75μL of 10mM dNTP, 0.5μL of Herculase II Fusion DNA Polymerase) was added in each PCR reaction (total 50μL) and incubated in a thermocycler (95˚C 3 min; 14 cycles of 95˚C 30s, 72˚C (−0.5˚C/cycle) 45s, 72˚C 30s/kb; 20 cycles of 95˚C 30s, 65˚C 45s, 72˚C 30s/kb; 72˚C 5 min and 10˚C keep). The fused product was gel purified in 20μL H_2O and inserted into pCR-Blunt II-TOPO vector (ThermoFisher Scientific 450245; 4μL gel purified DNA, 1μL salt solution, and 1μL TOPO vector were incubated for 5 min at RT; 5μL reaction was transformed in 50μL One Shot TOP10 Chemically Competent *E. coli* (ThermoFisher Scientific C404010) and cultured on a LB plate with 50μg/mL kanamycin). The fused HP2-L fragment was subcloned into the HP2-S plasmid (amplified by long template (>10kb) PCR: 50μL Herculase PCR mixture was incubated in a thermocycler (92˚C 2 min; 10 cycles of 92˚C 20s, 55˚C 20s, 68˚C 30s/kb; 20 cycles of 92˚C 20s, 55˚C 20s, 68˚C 30s/kb +20s/cycle; 68˚C 8 min and 10˚C keep)) using In-Fusion cloning. The PhiC31 integrase-mediated integration was conducted by BestGene Inc. The pUAST construct with RNAi resistant HP2-S is inserted into the VK27 site on 3R (BDSC 9744; y^1 w^{1118}; *Pbac{*y^+*-attP-9A}VK00027*). The pUAST construct with RNAi resistant HP2-L is inserted into the attP2 site on 3L (BDSC 8622; y^1 w^{67c23}; *P{*$y^{+t7.7}$*=CaryP}attP2*). Both constructs were balanced with TM3.

Analysis of spermatocyte-enriched DNA binding proteins

The list of proteins annotated as transcription factors or as containing a DNA binding domain were obtained from FlyBase. The Fly Cell Atlas testis dataset[1] was used to identify spermatocyte-enriched genes using the FindMarkers tool in Seurat v5.1, with spermatocytes defined as per the previous annotation. Bona fide markers were considered those with an

adjusted p-value < 1 x 10^{-9}. These lists were then intersected to obtain a catalog of putative transcription factors in spermatocytes.

Comparison of transcribed and translated protein-coding genes

Mass-spec data[18] was sorted by annotated "protein groups", with any protein group with a specific corresponding gene ID and at least one peptide across in all three adult testis replicates considered "translated". Genes were considered transcribed if they had an average expression of >=0.1 ln (UMIs-per-10,000 + 1) across the entire testis sequencing dataset. These lists were intersected to find genes transcribed, translated, or neither.

Identification of transcribed transposons and lncRNAs

We generated a new reference file that contains both DM6 and the consensus sequences of *Drosophila* transposons (https://github.com/bergmanlab/drosophila-transposons). The Fly Cell Atlas testis dataset was then remapped to this new reference file; processed, dimensionality reduced, and clustered according to previous parameters[1]; and annotations were transferred from the previous publication. lncRNAs, as identified in DM6, or transposons, as identified in the consensus file, were considered "expressed" in spermatocytes if they had an average expression of >=15 ln (UMIs-per-10,000 + 1) across all spermatocytes.

References

1. A. A. Raz, G. S. Vida, S. R. Stern, S. Mahadevaraju, J. M. Fingerhut, J. M. Viveiros, S. Pal, J. R. Grey, M. R. Grace, C. W. Berry, H. Li, J. Janssens, W. Saelens, Z. Shao, C. Hu, Y. M. Yamashita, T. Przytycka, B. Oliver, J. A. Brill, H. Krause, E. L. Matunis, H. White-Cooper, S. DiNardo, M. T. Fuller, Emergent dynamics of adult stem cell lineages from single nucleus and single cell RNA-Seq of *Drosophila* testes. *eLife*. **12**, e82201 (2023).
2. K. Wen, L. Yang, T. Xiong, C. Di, D. Ma, M. Wu, Z. Xue, X. Zhang, L. Long, W. Zhang, J. Zhang, X. Bi, J. Dai, Q. Zhang, Z. J. Lu, G. Gao, Critical roles of long noncoding RNAs in *Drosophila* spermatogenesis. *Genome Research*. **26**, 1233–1244 (2016).
3. W. K. Mills, Y. C. G. Lee, A. M. Kochendoerfer, E. M. Dunleavy, G. H. Karpen, RNA from a simple-tandem repeat is required for sperm maturation and male fertility in *Drosophila melanogaster*. *eLife*. **8**, e48940 (2019).
4. M. A. Lawlor, W. Cao, C. E. Ellison, A transposon expression burst accompanies the activation of Y-chromosome fertility genes during *Drosophila* spermatogenesis. *Nature Communications* **12**, 6854 (2021).
5. M. Soumillon, A. Necsulea, M. Weier, D. Brawand, X. Zhang, H. Gu, P. Barthès, M. Kokkinaki, S. Nef, A. Gnirke, M. Dym, B. de Massy, T. S. Mikkelsen, H. Kaessmann, Cellular source and mechanisms of high transcriptome complexity in the mammalian testis. *Cell Reports*. **3**, 2179–2190 (2013).
6. Y. Chen, Y. Zheng, Y. Gao, Z. Lin, S. Yang, T. Wang, Q. Wang, N. Xie, R. Hua, M. Liu, J. Sha, M. D. Griswold, J. Li, F. Tang, M.-H. Tong, Single-cell RNA-seq uncovers dynamic processes and critical regulators in mouse spermatogenesis. *Cell Research* **28**, 879–896 (2018).
7. J. Guo, E. J. Grow, H. Mlcochova, G. J. Maher, C. Lindskog, X. Nie, Y. Guo, Y. Takei, J. Yun, L. Cai, R. Kim, D. T. Carrell, A. Goriely, J. M. Hotaling, B. R. Cairns, The adult human testis transcriptional cell atlas. *Cell Research*. **28**, 1141–1157 (2018).
8. D. Wang, B. Eraslan, T. Wieland, B. Hallström, T. Hopf, D. P. Zolg, J. Zecha, A. Asplund, L. Li, C. Meng, M. Frejno, T. Schmidt, K. Schnatbaum, M. Wilhelm, F. Ponten, M. Uhlen, J. Gagneur, H. Hahne, B. Kuster, A deep proteome and transcriptome abundance atlas of 29 healthy human tissues. *Molecular Systems Biology*. **15**, e8503 (2019).
9. J. E. Pintar, B. S. Schachter, A. B. Herman, S. Durgerian, D. T. Krieger, Characterization and localization of proopiomelanocortin messenger RNA in the adult rat testis. *Science* **225**, 632–634 (1984).

10. B. Xia, Y. Yan, M. Baron, F. Wagner, D. Barkley, M. Chiodin, S. Y. Kim, D. L. Keefe, J. P. Alukal, J. D. Boeke, I. Yanai, Widespread transcriptional scanning in the testis modulates gene evolution rates. *Cell*. **180**, 248-262 (2020).
11. H. Liu, J. Zhang, Higher germline mutagenesis of genes with stronger testis expressions refutes the transcriptional scanning hypothesis. *Molecular Biology and Evolution*. **37**, 3225–3231 (2020).
12. P. M. B. Walker, Origin of satellite DNA. *Nature* **229**, 306–308 (1971).
13. J. J. Yunis, W. G. Yasmineh, Heterochromatin, satellite DNA, and cell function. *Science* **174**, 1200–1209 (1971).
14. A. R. Lohe, A. J. Hilliker, P. A. Roberts, Mapping simple repeated DNA sequences in heterochromatin of *Drosophila melanogaster*. *Genetics*. **134**, 1149–1174 (1993).
15. C. Rathke, W. M. Baarends, S. Awe, R. Renkawitz-Pohl, Chromatin dynamics during spermiogenesis. *Biochimica et Biophysica Acta*. **1839**, 155–168 (2014).
16. B. Loppin, F. Berger, Histone variants: the nexus of developmental decisions and epigenetic memory. *Annual Review of Genetics* **54**, 121–149 (2020).
17. H. Li, J. Janssens, M. De Waegeneer, S. S. Kolluru, K. Davie, V. Gardeux, W. Saelens, F. P. A. David, M. Brbić, K. Spanier, J. Leskovec, C. N. McLaughlin, Q. Xie, R. C. Jones, K. Brueckner, J. Shim, S. G. Tattikota, F. Schnorrer, K. Rust, T. G. Nystul, Z. Carvalho-Santos, C. Ribeiro, S. Pal, S. Mahadevaraju, T. M. Przytycka, A. M. Allen, S. F. Goodwin, C. W. Berry, M. T. Fuller, H. White-Cooper, E. L. Matunis, S. DiNardo, A. Galenza, L. E. O'Brien, J. A. T. Dow, H. Jasper, B. Oliver, N. Perrimon, B. Deplancke, S. R. Quake, L. Luo, S. Aerts, D. Agarwal, Y. Ahmed-Braimah, M. Arbeitman, M. M. Ariss, J. Augsburger, K. Ayush, C. C. Baker, T. Banisch, K. Birker, R. Bodmer, B. Bolival, S. E. Brantley, J. A. Brill, N. C. Brown, N. A. Buehner, X. T. Cai, R. Cardoso-Figueiredo, F. Casares, A. Chang, T. R. Clandinin, S. Crasta, C. Desplan, A. M. Detweiler, D. B. Dhakan, E. Donà, S. Engert, S. Floc'hlay, N. George, A. J. González-Segarra, A. K. Groves, S. Gumbin, Y. Guo, D. E. Harris, Y. Heifetz, S. L. Holtz, F. Horns, B. Hudry, R.-J. Hung, Y. N. Jan, J. S. Jaszczak, G. S. X. E. Jefferis, J. Karkanias, T. L. Karr, N. S. Katheder, J. Kezos, A. A. Kim, S. K. Kim, L. Kockel, N. Konstantinides, T. B. Kornberg, H. M. Krause, A. T. Labott, M. Laturney, R. Lehmann, S. Leinwand, J. Li, J. S. S. Li, K. Li, K. Li, L. Li, T. Li, M. Litovchenko, H.-H. Liu, Y. Liu, T.-C. Lu, J. Manning, A. Mase, M. Matera-Vatnick, N. R. Matias, C. E. McDonough-Goldstein, A. McGeever, A. D. McLachlan, P. Moreno-Roman, N. Neff, M. Neville, S. Ngo, T. Nielsen, C. E. O'Brien, D. Osumi-Sutherland, M. N. Özel, I. Papatheodorou, M. Petkovic, C. Pilgrim, A. O. Pisco, C. Reisenman, E. N. Sanders, G. dos Santos, K. Scott, A. Sherlekar, P. Shiu, D.

Sims, R. V. Sit, M. Slaidina, H. E. Smith, G. Sterne, Y.-H. Su, D. Sutton, M. Tamayo, M. Tan, I. Tastekin, C. Treiber, D. Vacek, G. Vogler, S. Waddell, W. Wang, R. I. Wilson, M. F. Wolfner, Y.-C. E. Wong, A. Xie, J. Xu, S. Yamamoto, J. Yan, Z. Yao, K. Yoda, R. Zhu, R. P. Zinzen, Fly Cell Atlas: A single-nucleus transcriptomic atlas of the adult fruit fly. *Science.* **375**, eabk2432 (2022).

18. S. M. K. Gärtner, T. Hundertmark, H. Nolte, I. Theofel, Z. Eren-Ghiani, C. Tetzner, T. B. Duchow, C. Rathke, M. Krüger, R. Renkawitz-Pohl, Stage-specific testes proteomics of *Drosophila melanogaster* identifies essential proteins for male fertility. *European Journal of Cell Biology*. **98**, 103–115 (2019).
19. M. Jagannathan, N. Warsinger-Pepe, G. J. Watase, Y. M. Yamashita, Comparative analysis of satellite DNA in the *Drosophila melanogaster* species complex. *G3 Genes|Genomes|Genetics*. **7**, 693–704 (2017).
20. K. H. Wei, S. E. Lower, I. V. Caldas, T. J. S. Sless, D. A. Barbash, A. G. Clark, Variable rates of simple satellite gains across the *Drosophila* phylogeny. *Molecular Biology and Evolution*. **35**, 925–941 (2018).
21. C. Chang, A. M. Larracuente, Heterochromatin-enriched assemblies reveal the sequence and organization of the *Drosophila melanogaster* Y chromosome. *Genetics*. **211**, 333–348 (2018).
22. S. Bonaccorsi, C. Pisano, F. Puoti, M. Gatti, Y chromosome loops in *Drosophila melanogaster*. *Genetics*. **120**, 1015–1034 (1988).
23. S. Bonaccorsi, A. Lohe, Fine mapping of satellite DNA sequences along the Y chromosome of *Drosophila melanogaster*: relationships between satellite sequences and fertility factors. *Genetics* **129**, 177–189 (1991).
24. J. M. Fingerhut, J. V. Moran, Y. M. Yamashita, Satellite DNA-containing gigantic introns in a unique gene expression program during *Drosophila* spermatogenesis. *PLOS Genetics*. **15**, e1008028 (2019).
25. C. D. Shaffer, G. E. Stephens, B. A. Thompson, L. Funches, J. A. Bernat, C. A. Craig, S. C. R. Elgin, Heterochromatin protein 2 (HP2), a partner of HP1 in *Drosophila* heterochromatin. *Proceedings of the National Academy of Sciences*. **99**, 14332–14337 (2002).
26. G. E. Stephens, E. E. Slawson, C. A. Craig, S. C. R. Elgin, Interaction of heterochromatin protein 2 with HP1 defines a novel HP1-binding domain. *Biochemistry*. **44**, 13394–13403 (2005).
27. The modENCODE Consortium et al., Identification of functional elements and regulatory circuits by *Drosophila* modENCODE. *Science*. **330**, 1787–1797 (2010).

28. M. M. Kudron, A. Victorsen, L. Gevirtzman, L. W. Hillier, W. W. Fisher, D. Vafeados, M. Kirkey, A. S. Hammonds, J. Gersch, H. Ammouri, M. L. Wall, J. Moran, D. Steffen, M. Szynkarek, S. Seabrook-Sturgis, N. Jameel, M. Kadaba, J. Patton, R. Terrell, M. Corson, T. J. Durham, S. Park, S. Samanta, M. Han, J. Xu, K.-K. Yan, S. E. Celniker, K. P. White, L. Ma, M. Gerstein, V. Reinke, R. H. Waterston, The ModERN resource: genome-wide binding profiles for hundreds of *Drosophila* and *Caenorhabditis elegans* transcription factors. *Genetics* **208**, 937–949 (2018).
29. C. D. Shaffer, G. Cenci, B. Thompson, G. E. Stephens, E. E. Slawson, K. Adu-Wusu, M. Gatti, S. C. R. Elgin, The large isoform of *Drosophila melanogaster* heterochromatin protein 2 plays a critical role in gene silencing and chromosome structure. *Genetics*. **174**, 1189–1204 (2006).
30. S. E. Castel, R. A. Martienssen, RNA interference in the nucleus: roles for small RNAs in transcription, epigenetics and beyond. *Nature Reviews Genetics* **14**, 100–112 (2013).
31. R. A. Hoskins, J. W. Carlson, K. H. Wan, S. Park, I. Mendez, S. E. Galle, B. W. Booth, B. D. Pfeiffer, R. A. George, R. Svirskas, M. Krzywinski, J. Schein, M. C. Accardo, E. Damia, G. Messina, M. Méndez-Lago, B. de Pablos, O. V. Demakova, E. N. Andreyeva, L. V. Boldyreva, M. Marra, A. B. Carvalho, P. Dimitri, A. Villasante, I. F. Zhimulev, G. M. Rubin, G. H. Karpen, S. E. Celniker, The Release 6 reference sequence of the *Drosophila melanogaster* genome. *Genome Research* **25**, 445–458 (2015).
32. K. H. Wei, J. K. Grenier, D. A. Barbash, A. G. Clark, Correlated variation and population differentiation in satellite DNA abundance among lines of *Drosophila melanogaster*. *Proceedings of the National Academy of Sciences*. **111**, 18793–18798 (2014).
33. X. Wei, D. G. Eickbush, I. Speece, A. M. Larracuente, Heterochromatin-dependent transcription of satellite DNAs in the *Drosophila melanogaster* female germline. *eLife* **10**, e62375 (2021).
34. M. V. Doren, A. L. Williamson, R. Lehmann, Regulation of zygotic gene expression in *Drosophila* primordial germ cells. *Current Biology* **8**, 243–246 (1998).
35. D. Chen, D. M. McKearin, A discrete transcriptional silencer in the gene determines asymmetric division of the *Drosophila* germline stem cell. *Development* **130**, 1159–1170 (2003).
36. E. Rebollo, S. Llamazares, J. Reina, C. Gonzalez, Contribution of noncentrosomal microtubules to spindle assembly in *Drosophila* spermatocytes. *PLoS Biology* **2**, e8 (2004).
37. Y. Shindo, A. A. Amodeo, Dynamics of free and chromatin-bound histone H3 during early embryogenesis. *Current Biology* **29**, 359-366 (2019).

38. J. I. Park, G. W. Bell, Y. M. Yamashita, Derepression of Y-linked multicopy protamine-like genes interferes with sperm nuclear compaction in *D. melanogaster*. *Proceedings of the National Academy of Sciences* **120**, e2220576120 (2023).
39. S. Misra, M. A. Crosby, C. J. Mungall, B. B. Matthews, K. S. Campbell, P. Hradecky, Y. Huang, J. S. Kaminker, G. H. Millburn, S. E. Prochnik, C. D. Smith, J. L. Tupy, E. J. Whitfield, L. Bayraktaroglu, B. P. Berman, B. R. Bettencourt, S. E. Celniker, A. D. de Grey, R. A. Drysdale, N. L. Harris, J. Richter, S. Russo, A. J. Schroeder, S. Shu, M. Stapleton, C. Yamada, M. Ashburner, W. M. Gelbart, G. M. Rubin, S. E. Lewis, Annotation of the *Drosophila melanogaster* euchromatic genome: a systematic review. *Genome Biology* **3**, 12 (2002).
40. V. Mérel, M. Boulesteix, M. Fablet, C. Vieira, Transposable elements in *Drosophila*. *Mobile DNA* **11**, 23 (2020).

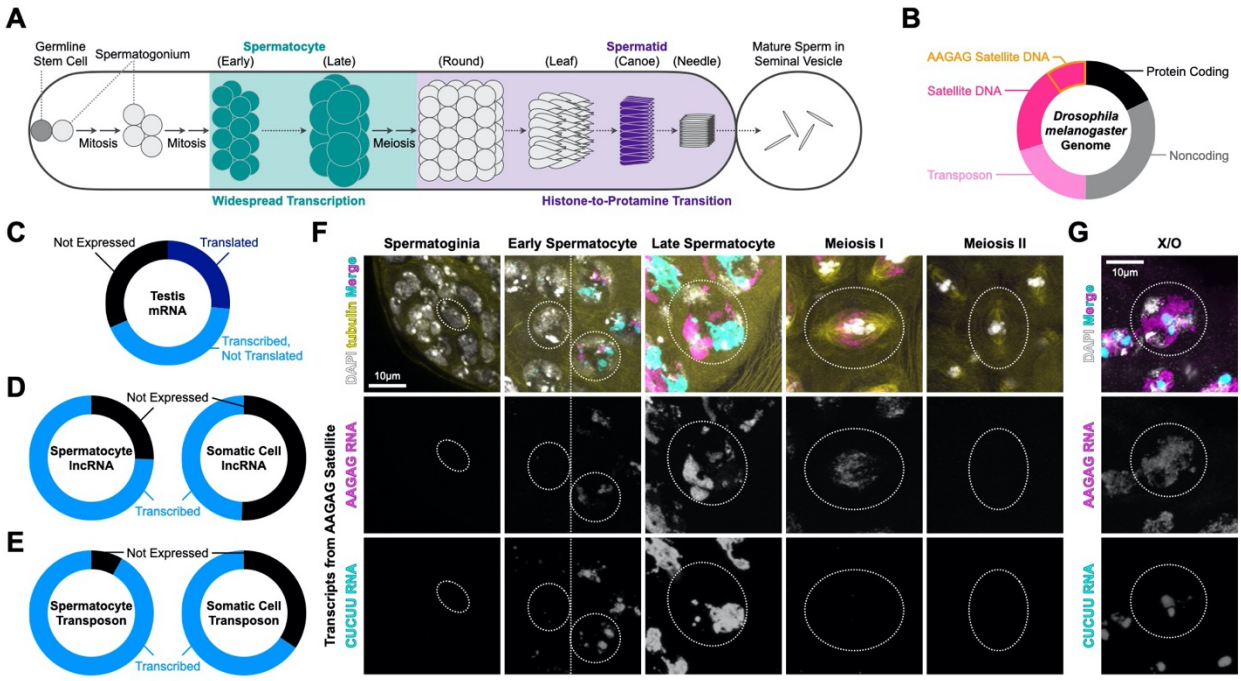

Figure 1: *Drosophila* spermatocytes exhibit widespread transcription

(A) Schematics of *Drosophila* spermatogenesis. Germline stem cells at the apical tip of the testis (left in the cartoon) produce differentiating spermatogonia, which divide four times before becoming spermatocytes. While spermatocytes grow in size, they exhibit high-complexity transcriptome, with many coding and noncoding transcripts. After meiosis, spermatid nuclei undergo morphological changes through round, leaf, canoe, and needle stages, during which histone is replaced by protamine. Mature sperm are stored in seminal vesicles and prepared for ejaculation.

(B) Composition of *Drosophila melanogaster* genome. Approximately 20% are protein coding sequences, 30% noncoding sequences, 20% transposons, and 30% satellite DNA[14,21,39,40]. AAGAG satellite DNA typically occupies approximately 10% of the genome.

(C) Expression of protein coding genes (12,760 genes) in the *Drosophila* testis. Approximately 70% of total protein coding genes expressed (30% translated (dark blue), and 40% transcribed but not translated (blue)), while 30% are not expressed (black).

(D-E) Expression of lncRNAs (1764 genes) and transposons (122 transposons) in spermatocytes vs. somatic cells (somatic epithelia surrounding each cyst). Note that the RNA sequencing data[1] were obtained by polyA selection, thus cannot capture transcripts that are not polyadenylated.

(F) RNA FISH of AAGAG/CUCUU satellite transcripts in male germ cells in various stages of differentiation (germline stem cells/spermatogonia, spermatocytes, meiotic cells).

AAGAG/CUCUU satellite RNA is robustly transcribed in spermatocytes then disappear during meiotic divisions.

(G) RNA FISH of AAGAG/CUCUU satellite transcripts in the spermatocyte of X/O males lacking the Y chromosome.

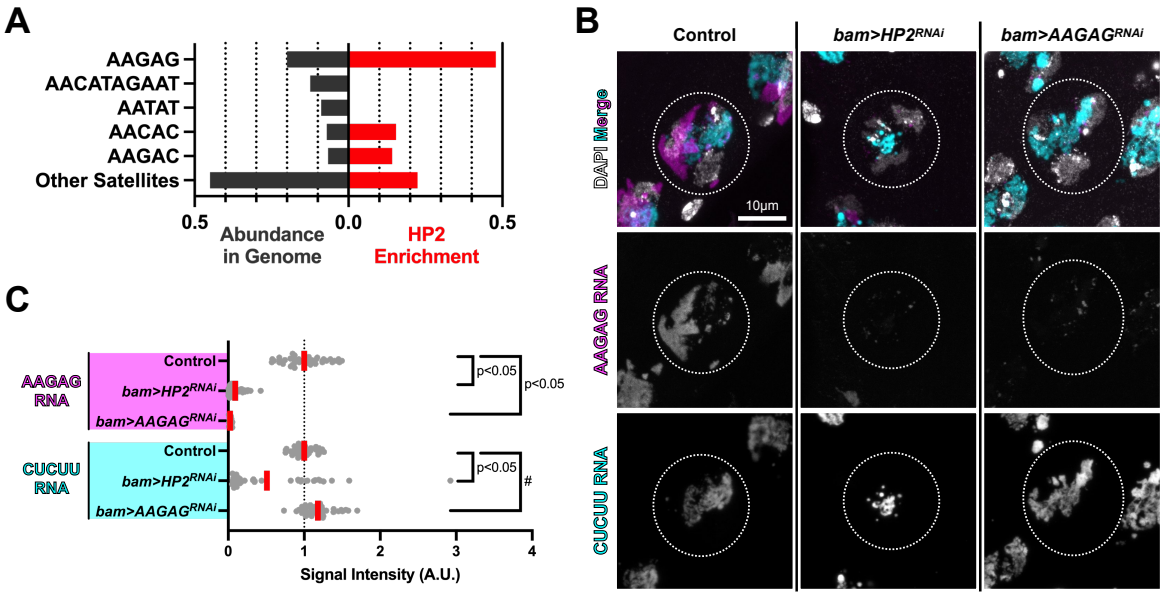

Figure 2: HP2 regulates transcription of AAGAG satellite DNA in spermatocytes

(A) Abundance of satellite DNA in the *Drosophila* genome calculated from the whole genome sequencing[20] (on the left) compared to HP2-ChIP-seq enrichment on satellite DNA (modENCODE ID: 5593)[27] (on the right). The data were analyzed using the k-Seek method[32] to quantify simple satellite repeat abundance from short-read sequencing.

(B) RNA FISH of AAGAG/CUCUU satellite transcripts in control, *bam>HP2*^{RNAi} and *bam>AAGAG*^{RNAi} spermatocytes. Spermatocyte nuclei are indicated by dotted circle.

(C) Relative signal intensities of AAGAG/CUCUU transcripts in control, *bam>HP2*^{RNAi} and *bam>AAGAG*^{RNAi} (n≥20 testes from each genotype). Red line: mean. The *p*-value is calculated by unpaired t test. #: CUCUU RNA was slightly but significantly ($p<0.05$) upregulated in *bam>AAGAG*^{RNAi} (Method)

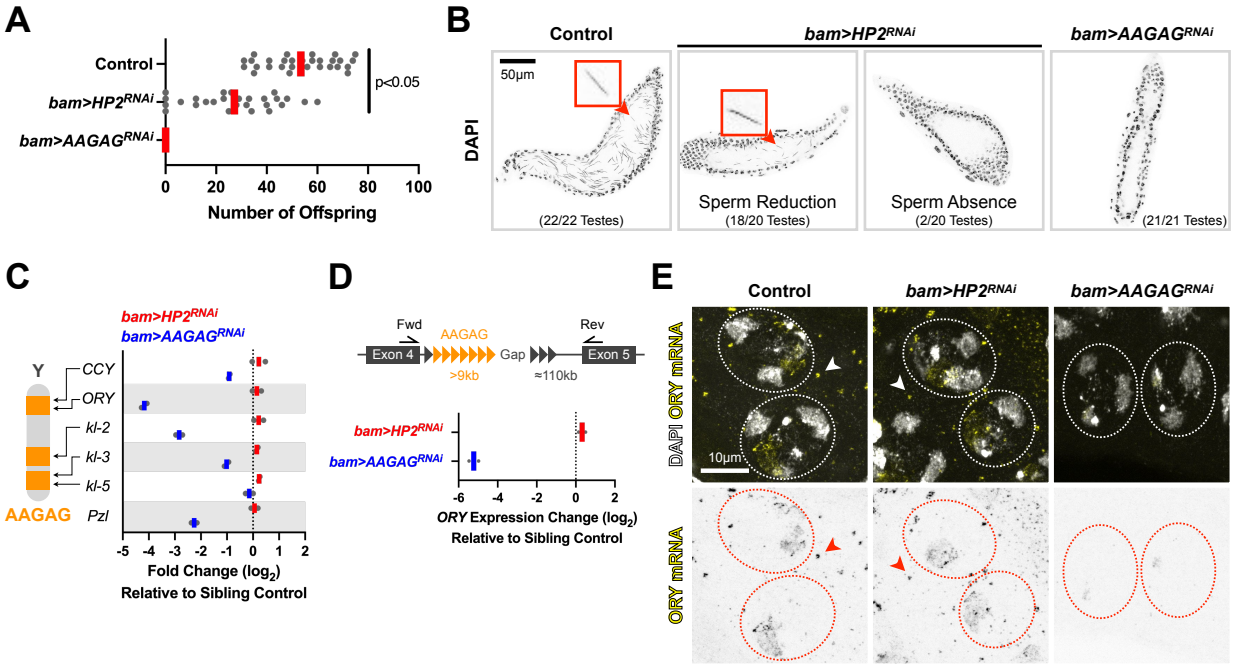

Figure 3: HP2 depletion leads to subfertility

(A) Fertility assay of wild type, *bam>HP2*^{RNAi} and *bam>AAGAG*^{RNAi} males. Each dot represents the number of offspring from a single mating pair (n≥27 from each genotype); red line, mean. The *p*-value is calculated by unpaired t test.

(B) Seminal vesicles of wild type, *bam>HP2*^{RNAi} and *bam>AAGAG*^{RNAi} males stained with DAPI. Only the seminal vesicle was cropped for clarity using Fiji/ImageJ. An example of sperm nucleus is marked with red.

(C) Cytological map of AAGAG satellite DNA and fertility genes on the Y chromosome[14,19,21]. *Pzl* is an autosomal gene with large intronic AAGAG satellite DNA (Figure S4). RT-qPCR using the primers to amplify the last exon of indicated genes in *bam>HP2*^{RNAi} and *bam>AAGAG*^{RNAi} compared to control with technical duplicates for each genotype.

(D) RT-qPCR using the primers to amplify exon-exon junction across AAGAG satellite DNA-containing introns of *ORY* gene with technical duplicates for each genotype.

(E) RNA FISH of *ORY* mRNA in spermatocytes in control, *bam>HP2*^{RNAi} and *bam>AAGAG*^{RNAi}. Cytoplasmic *ORY* mRNA granules (arrowheads) are formed in control and *bam>HP2*^{RNAi}, but not in *bam>AAGAG*^{RNAi}.

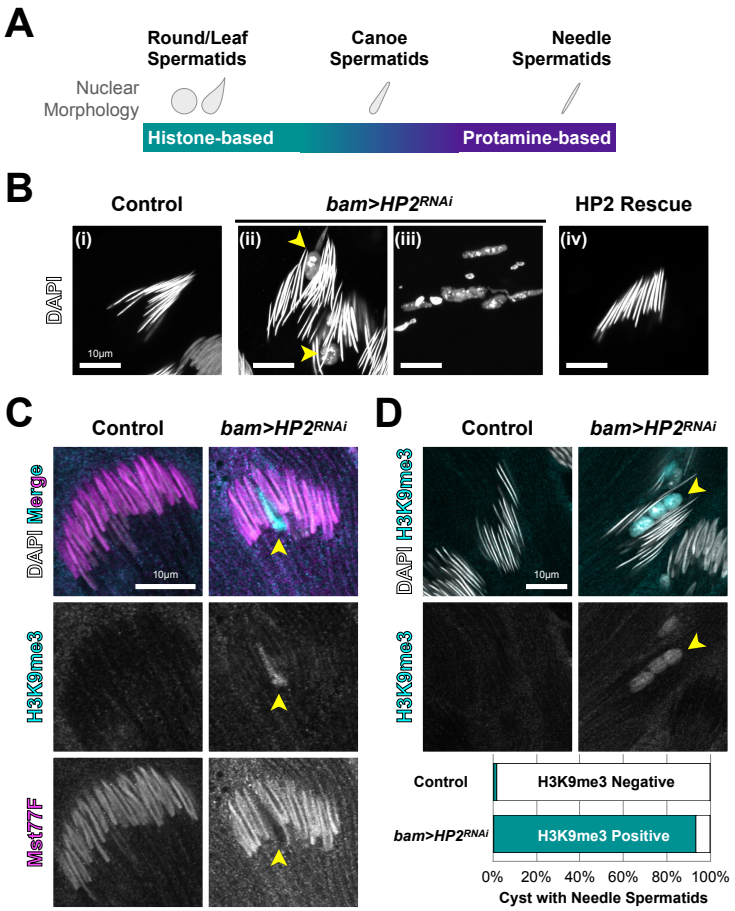

Figure 4: HP2 depletion leads to defective histone-to-protamine transition in spermatids

(A) Schematics of sperm development and histone-to-protamine transition. Histone-to-protamine transition occurs in the canoe stage spermatids.

(B) Needle stage spermatids in control and *bam>HP2*^{RNAi} animals, and *bam>HP2*^{RNAi} animals with HP2 rescue construct (RNAi-resistant HP2-S transgene) stained with DAPI. Spermatid nuclei with defective sperm DNA compaction is indicated by arrowheads in ii. In some cysts (iii), all spermatids within a cyst failed to compact DNA.

(C) Immunofluorescence staining of H3K9me3 and Mst77F in canoe spermatids from control and *bam>HP2*^{RNAi} animals. Arrowheads indicate a spermatid nucleus that failed to undergo histone-to-protamine transition (n=15 testes for each genotype).

(D) Immunofluorescence staining of H3K9me3 in needle spermatids from control and *bam>HP2*^{RNAi} animals. Arrowhead indicates spermatid nuclei in *bam>HP2*^{RNAi} animals that failed to undergo sperm DNA compaction and retained the H3K9me3 histone mark. Frequencies of cysts with H3K9me3 histone mark in needle stage spermatid in control and *bam>HP2*^{RNAi} animals is shown. (n≥60 cysts from ≥10 testes for each genotype).

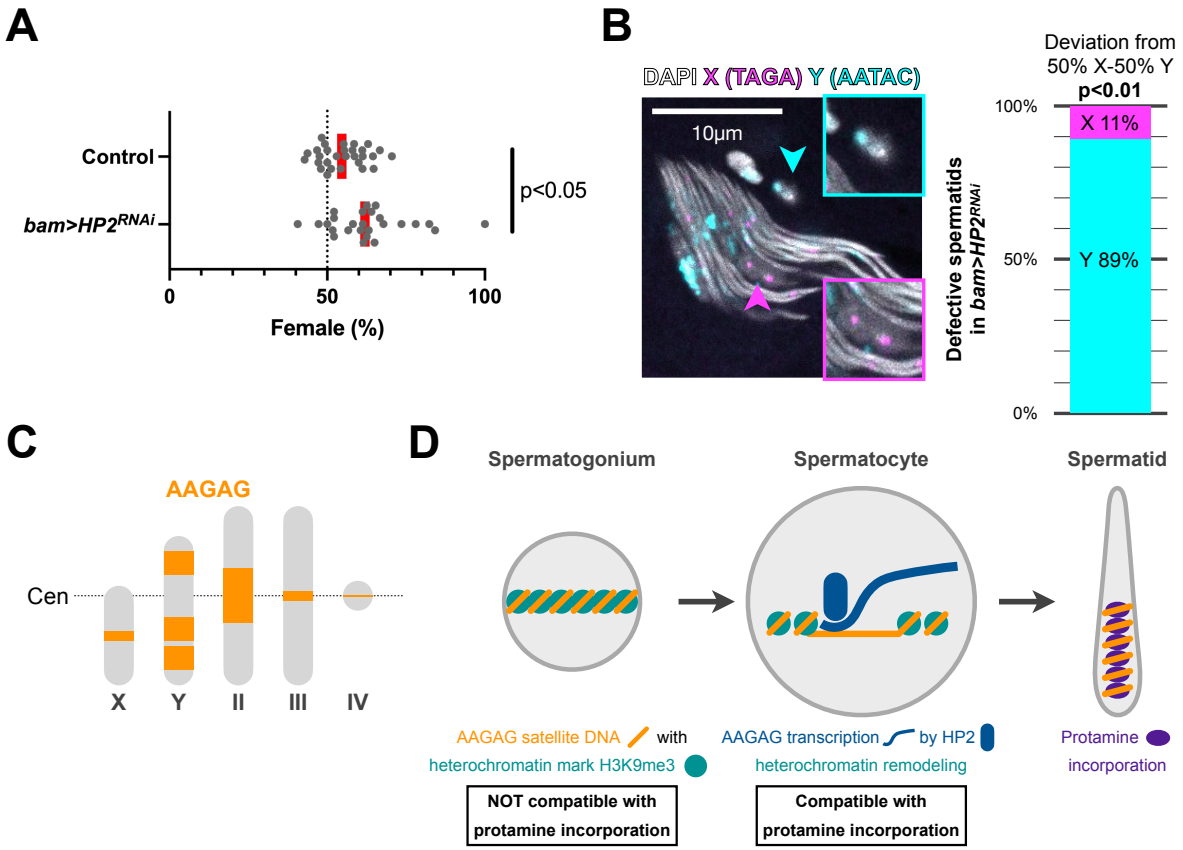

Figure 5: HP2 depletion preferentially impacts Y-chromosome containing spermatids

(A) Sex ratio of offspring of control vs. *bam>HP2*^{RNAi} males. Each dot represents the sex ratio of offspring from a single mating pair in Figure 3B (n≥28 from each genotype); red line, geometric mean. The *p*-value is calculated by unpaired t test.

(B) DNA FISH on needle stage spermatids in *bam>HP2*^{RNAi} spermatids using X- and Y-specific satellite DNA X: TAGA satellite DNA. Y: AATAC satellite DNA. The frequency of defective spermatids with X vs. Y chromosome is shown (n=37 spermatids from 16 testes). The *p*-value is calculated by chi square test for goodness of fit for deviations from 50% X and 50% Y.

(C) Schematics of *Drosophila melanogaster* karyotype with AAGAG satellite DNA location (orange block, size is proportional to the estimate[14]). Large AAGAG satellite blocks are found in intergenic regions of the Y chromosome and pericentromeric region of the chromosome II.

(D) Model for the functional significance of transcription.

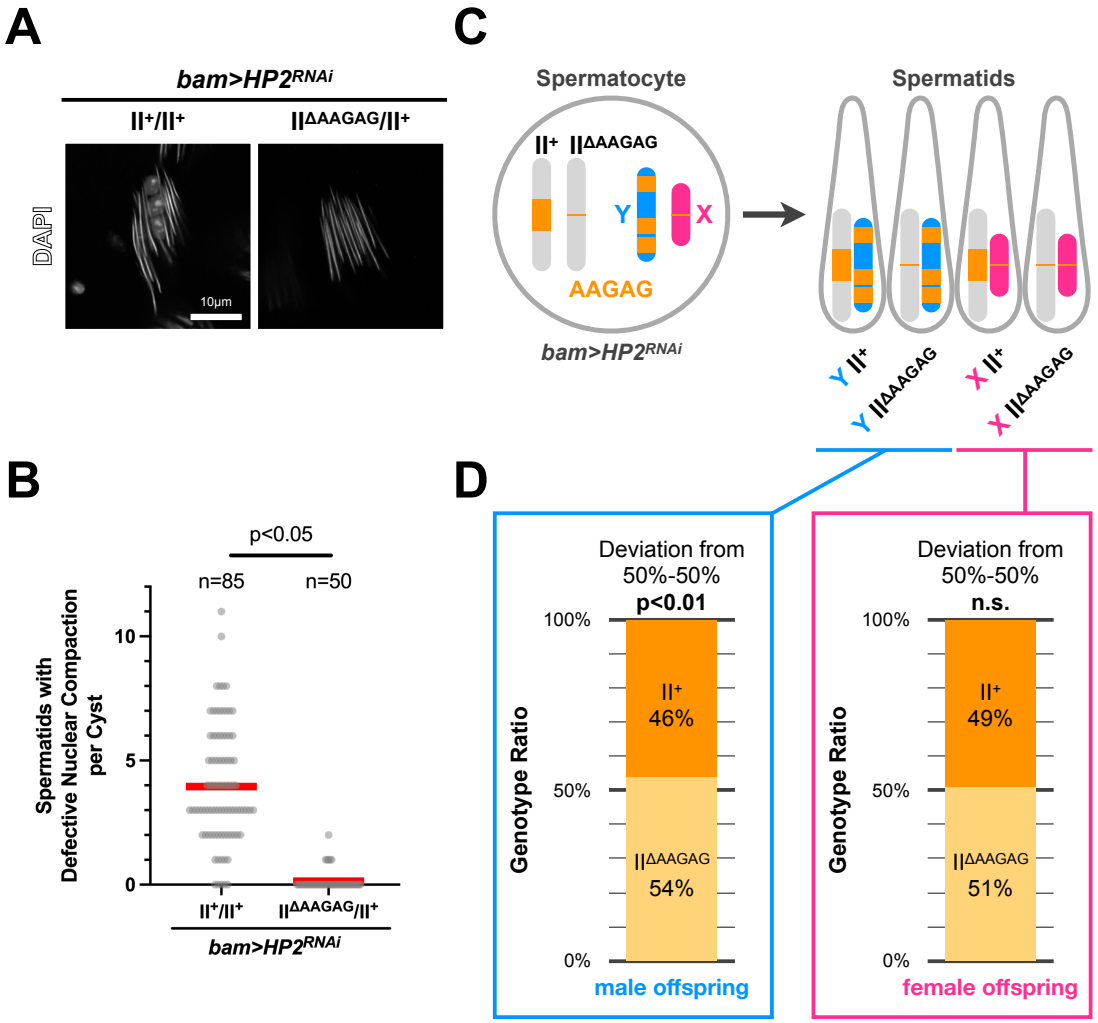

Figure 6: Chromosome II with minimal amount of AAGAG satellite DNA is more resistant to HP2 depletion

(A) Needle stage spermatids stained with DAPI from *bam>HP2*^{RNAi} animals with animals with indicated chromosome II genotypes (II^{+}/II^{+} and II$^{\Delta AAGAG}$/II^{+}).

(B) The number of spermatids with defective sperm DNA compaction per cyst from *bam>HP2*^{RNAi} animals with indicated chromosome II genotypes (II^{+}/II^{+} and II$^{\Delta AAGAG}$/II^{+}). n = the number of cysts from ≥10 testes for each genotype. The *p*-value is calculated by unpaired t test.

(C) Genotype of spermatids generated from X/Y; II+/II$^{\Delta AAGAG}$ (*bam>HP2*^{RNAi}) spermatocytes.

(D) The frequency of the offspring inherited chromosome II+ or II$^{\Delta AAGAG}$ from the X/Y; II+/II$^{\Delta AAGAG}$ *bam>HP2*^{RNAi} fathers (n=1145 male animals; n=296 female animals). The *p*-value is calculated by chi square test for goodness of fit for deviations from 50% II^{+} and 50% II$^{\Delta AAGAG}$.

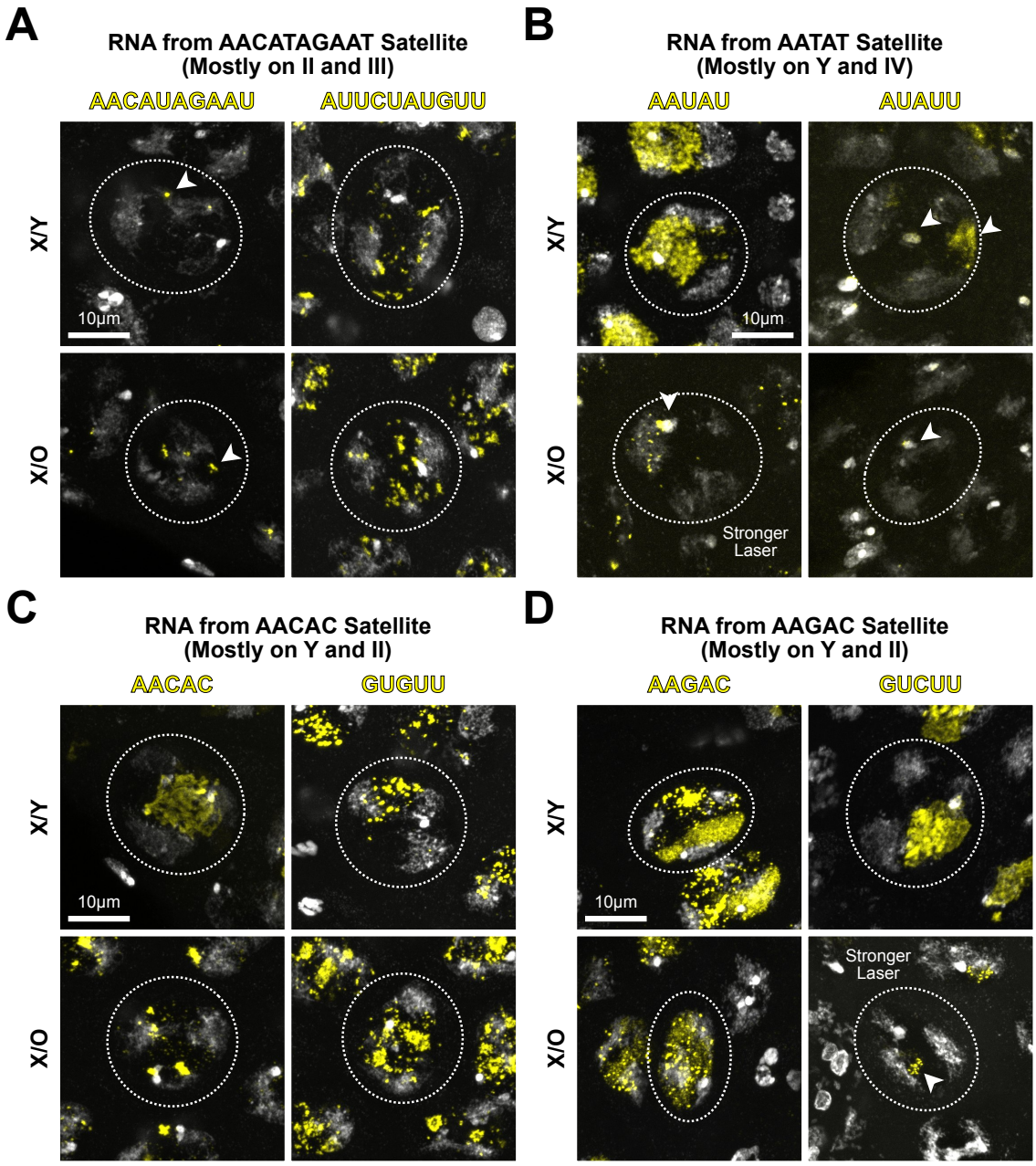

Supplementary Figure 1: A broad range of satellite DNAs are also transcribed in spermatocytes

(A-D) RNA FISH of various satellite transcripts in X/Y and X/O spermatocytes. Weakly transcribed loci are highlighted with white arrowheads. Transcripts of indicated satellite DNA are shown in yellow, with DAPI in gray.

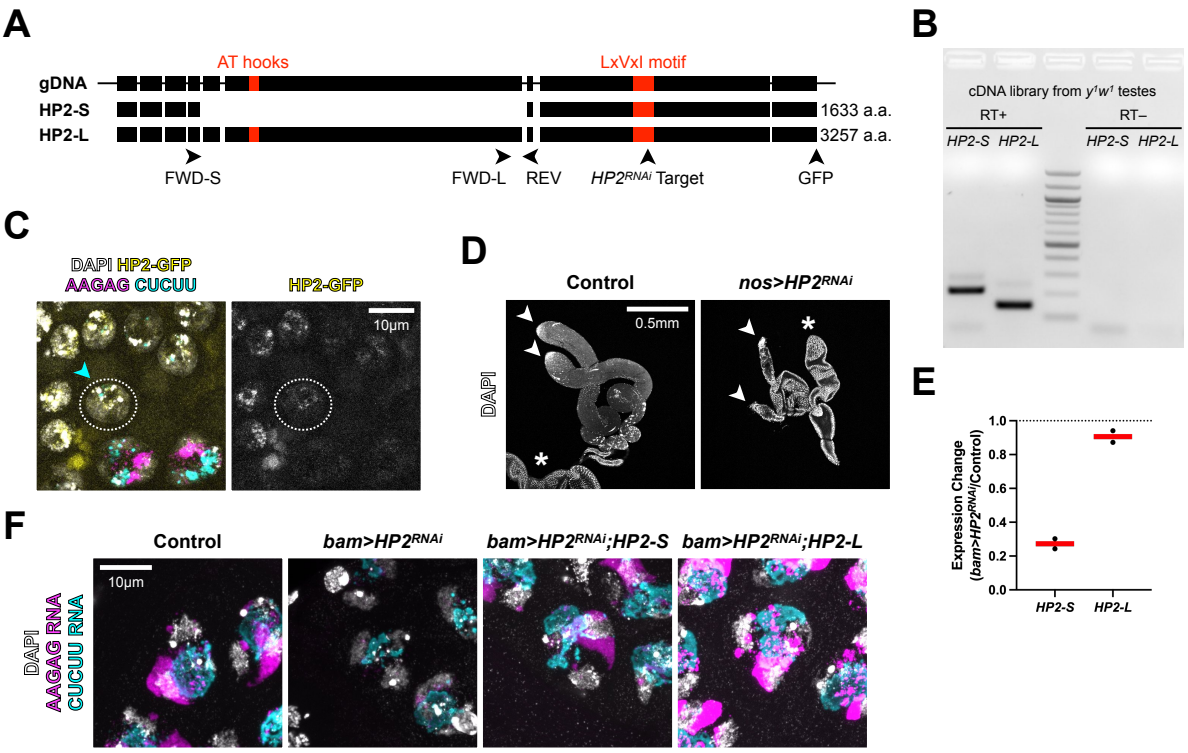

Supplementary Figure 2: Both HP2 isoforms can rescue the HP2 RNAi phenotype

(A) Schematics of the HP2 genomic sequence and the two isoforms (HP2-S and HP2-L). Black boxes are exons, ordered from 5' (left) to 3' (right), with introns, 5' upstream and 3' downstream sequences represented as a line. Satellite DNA interacting domain (two AT hooks, GRP) and HP1-interacting domain (LxVxI motif, LCVKI) are shown in red. Locations of primers used for panels B and E, GFP-tag used for panel C, and *HP2*^{RNAi} target sequence (CAGGAGAGGAATGAAGAACAA) are shown with arrowheads.

(B) RT-PCR to detect long and short isoforms of HP2 in the testis.

(C) AAGAG/CUCUU RNA FISH on HP2-GFP testis. Early spermatocyte nuclus is indicated by dotted circle, and CUCUU RNA is indicated by arrowhead.

(D) The testes from control vs. *nos>HP2*^{RNAi} (arrowheads) stained with DAPI. Asterisks show accessory glands.

(E) RT-qPCR using the primer sets for each HP2 isoform in *bam>HP2*^{RNAi} compared to control with technical duplicates. *bam>HP2*^{RNAi} reduced HP2-S expression, but not HP2-L, suggesting that HP2-S is the dominant isoform in spermatocytes.

(F) RNA FISH of AAGAG/CUCUU satellite transcripts in control, *bam>HP2*^{RNAi}, and *bam>HP2*^{RNAi} with HP2 rescue construct (designed to be resistant to RNAi, Method).

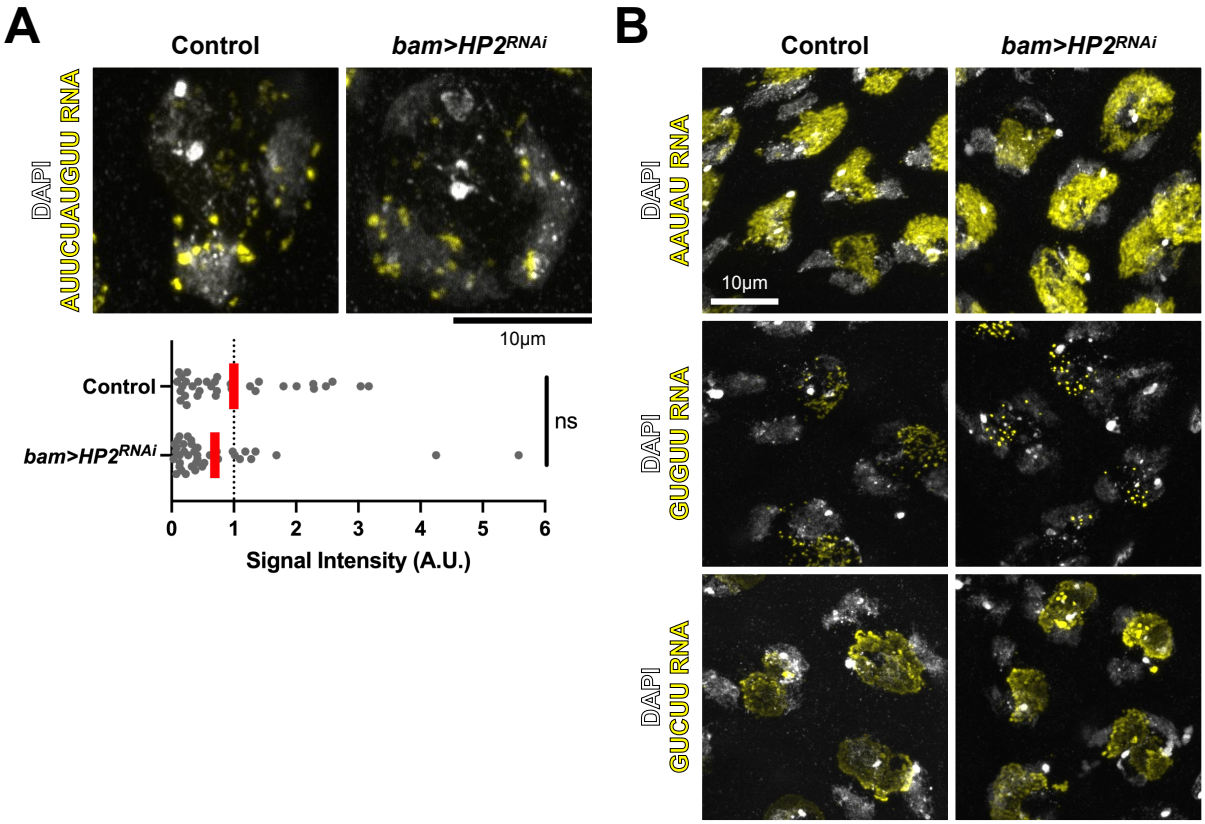

Supplementary Figure 3: HP2 depletion has little effect on transcripts from other satellite DNA than AAGAG.

(A) RNA FISH (top) and relative signal intensities (bottom) of AUUCUACGCC RNA in control and *bam>HP2*^{RNAi} spermatocytes (n≥33 spermatocytes from ≥14 testes from each genotype). Red line, mean. The *p*-value is calculated by unpaired t test, and the *p*-value of less than 0.05 is judged as statistically significant. ns, not significant.

(B) RNA FISH of AAUAU, GUGUU, and GUCUU RNA in control and *bam>HP2*^{RNAi} spermatocytes.

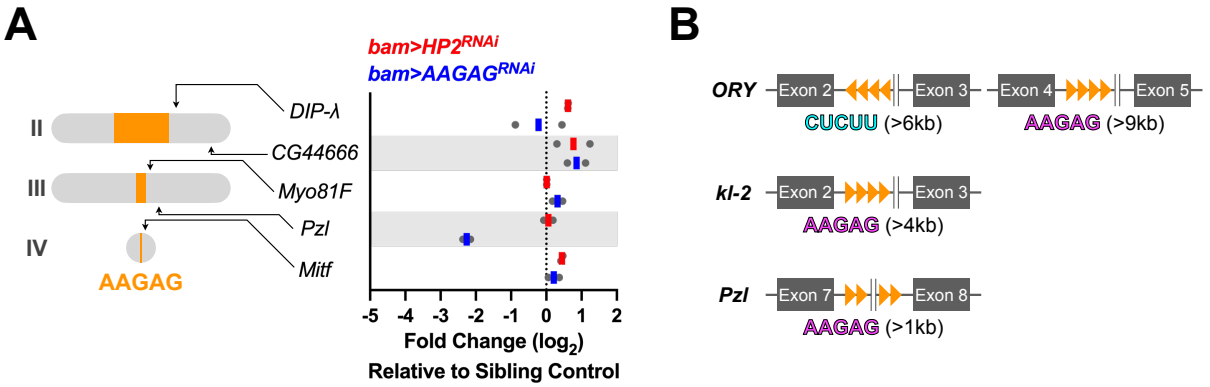

Supplementary Figure 4: Genomic location of AAGAG satellite DNA

(A) Cytological map of AAGAG satellite DNA[14,19] (orange) and genes with gaps in the assembly[31], which are potential sites for intronic AAGAG. RT-qPCR using the primers to amplify the last exon of indicated genes in *bam>HP2*^{RNAi} and *bam>AAGAG*^{RNAi} compared to control with technical duplicates for each genotype.

(B) Intronic AAGAG satellite DNA in *ORY*, *kl*-2, and *Pzl* genes. AAGAG satellite repeats are found next to the gaps in the genome assembly.

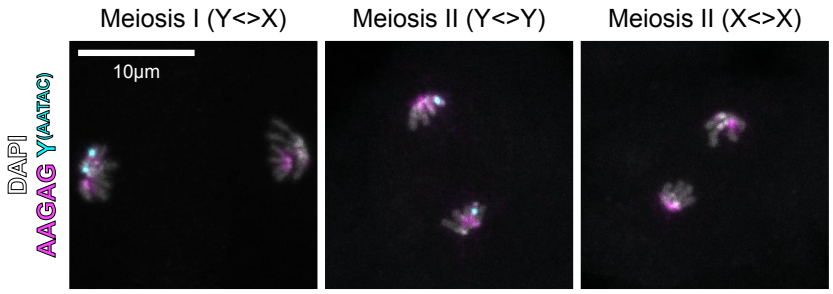

Supplementary Figure 5: Meiotic chromosome segregation appears normal in HP2 depletion

DNA FISH on meiotic chromosome spread from the adult testis using AAGAG and Y-specific AATAC satellite DNA probes (n=20 testes).

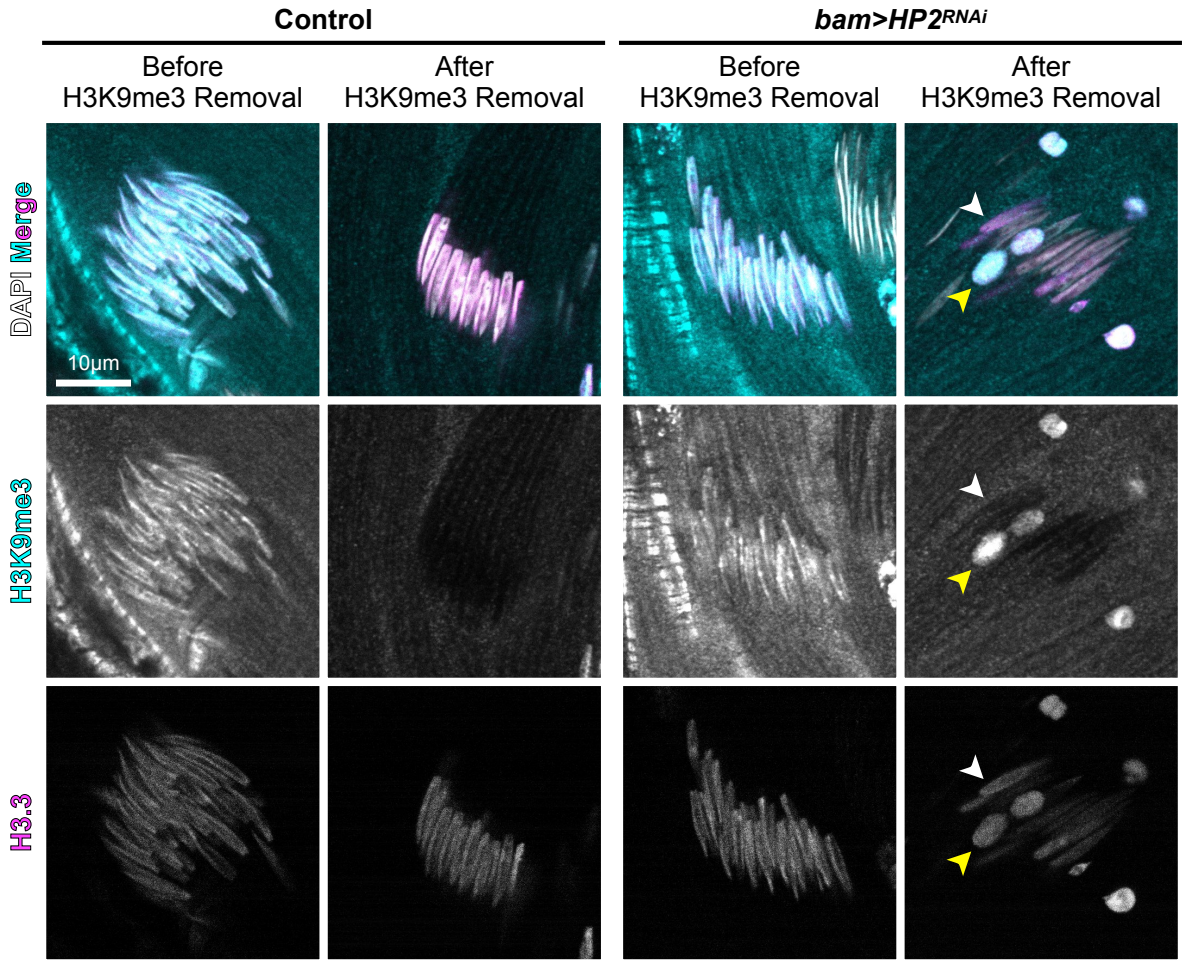

Supplementary Figure 6: Orderly remodeling of spermatid chromatin is compromised in *bam>HP2^{RNAi}*.

Immunofluorescence staining of spermatids in control vs. *bam>HP2^{RNAi}* with H3K9me3 and H3.3-Dendra2 during spermatid chromatin remodeling. White arrowheads indicate spermatid nuclei that successfully removed H3K9me3, and yellow arrowheads spermatid nuclei that retained H3K9me3 and failed to undergo sperm DNA compaction (n=15 testes for each genotype).

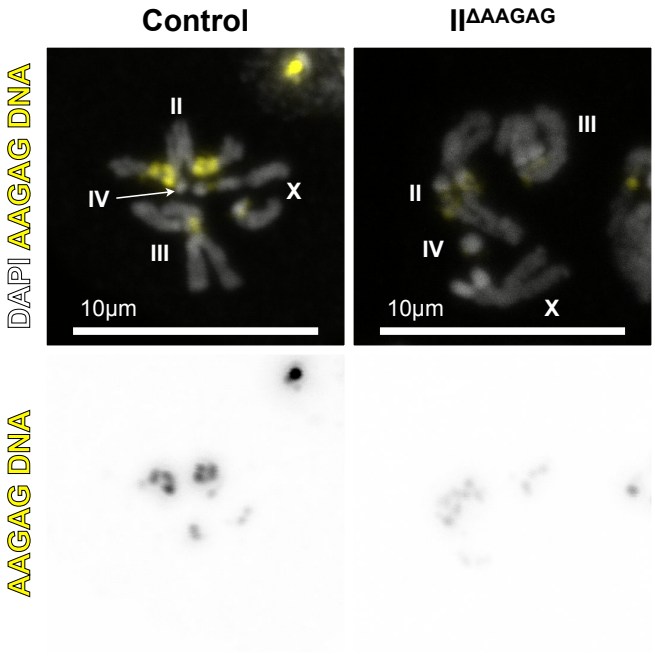

Supplementary Figure 7: Little AAGAG is present on the II$^{\Delta AAGAG}$ chromosome

DNA FISH on mitotic chromosome spread from the larval brain using the AAGAG satellite DNA probe. One of the wild-derived strain (I16) carries little AAGAG satellite on the chromosome II (II$^{\Delta AAGAG}$) than the control (B52)[32].